Construction of mutant TNF phage library (Gene Shuffling Library). The pCANTAB phagemid vector encoding a lysine-deficient mutant TNF which was created previously was used as a template for library construction [15]. First, two types of phage libraries, displaying mutant TNFs containing random substitutions of amino acid residues at positions 29, 31, 32, 145, 146 and 147 (Library I), and at positions 84, 85, 86, 87, 88 and 89 (Library II), were prepared using polymerase chain reaction (PCR) as described earlier [11,12]. Each library was then subjected to two rounds of panning against TNFR1 to concentrate TNFR1-specific high-affinity mutant TNFs. Next, we purified all plasmids from each concentrated libraries. These two pools of purified plasmids were digested with the restrict enzymes (*Ppu*MI, *Bst*EII), DNA inserts were purified and then ligated to a pY03′ phagemid vector to construct a randomized library (Shuffling Library A) that contained mutations at twelve different amino acid residues (see Fig. 1). We also prepared a second randomized library (Shuffling Library B) by following the same protocol and using TNFR2 for panning.

Competitive ELISA. Inhibition of wtTNF binding to the TNFR1 and TNFR2 by a TNFR1 or TNFR2-selective mutant was measured using ELISA as described previously [16]. The wtTNF-FLAG, a FLAG tag fusion protein of human TNF [16], was used as a marker protein. Briefly, the immune assay plates (NUNC, Roskilde, Denmark) were coated with 5 μg/ml goat anti-human IgG antibody (MP Biomedicals, Aurora, OH) and incubated with 0.2 μg/ml of either the human TNFR1 or the human TNFR2. After blocking the non-specific binding sites, a pre-made mixture containing 100 ng/ml of wtTNF-FLAG and various concentrations of a given TNF mutant was added to the wells. After 2 h of incubation at room temperature, the wells were washed. Next, 0.5 μg/ml biotinylated anti-FLAG M2 antibody was added to each well and then the plate was incubated for an additional period of 2 h at room temperature. Wells were washed and then incubated with the horseradish peroxidase-coupled streptavidin (Zymed Lab. Inc., South San Francisco, CA) for 30 min at room temperature. The remaining bound wtTNF-FLAG was quantified as described above.

Assay for cytotoxicity mediated via TNFR1 and TNFR2. To measure cytotoxicity mediated via the TNFR1, HEp-2 cells (4×10^4 cells/well) were cultured in 96-well plates (NUNC, Roskilde, Denmark) in presence of a given TNF mutant, serially diluted human wtTNF (Peprotech, Rocky Hill, NJ), and with 100 μg/ml cycloheximide for 18 h, and cytotoxicity was assessed by using the methylene blue assay as described previously [17]. To measure cytotoxicity mediated via the TNFR2, hTNFR2/mFas-preadipocyte cells (1×10^4 cells/well) were cultured in the 96-well plates (NUNC) in presence of a given TNF mutant and serially diluted human wtTNF for 48 h, and then cell survival was determined by using the methylene blue assay.

Results and discussion

In this study, to overcome the barrier of limited transformation efficiency of *E. coli* in the preparation of high quality phage display libraries, we adopted a novel protein engineering technology in which amino acid residues at 12 different places were randomly substituted using a gene shuffling method to enhance the usefulness of the phage display technique.

Fig. 1 schematically summarizes the protocol used for constructing a novel TNF gene shuffling library. First, we prepared two phage libraries displaying mutant TNFs, in each of which six different amino acid residues (residues at positions 29, 3, 32, 145, 146 and 147 for Library I; residues at positions from 84 to 89 for Library II) present in the receptor binding site of TNF, previously identified by point mutation analysis and X-ray crystallography, were randomly substituted with other amino acid residues [11,12]. The phage libraries expressing mutant TNFs were constructed by two-step PCR as described in the Materials and methods. We confirmed that the phage Libraries I and II consisted of 8×10^6 and 6×10^6 independent clones, respectively (*data not shown*). Next, to enrich for TNFR1 binding mutants, we subjected each library to two rounds of panning using TNFR1 and recovered phage clones with high affinity to TNFR1. We used a gene shuffling method to construct the mutant TNF Shuffling Library A from these libraries, which consist of high affinity clones to TNFR1 (see Fig. 1). In the similar manner, we constructed the Shuffling Library B by carrying out panning using TNFR2. Amino acid analysis of eight randomly picked clones from each library revealed that each one of them was a mutant containing amino acid substitutions at 12 residues (*results not shown*). To concentrate TNFR1-selective mutant TNFs, the Shuffling Library A was subjected to two rounds of panning against TNFR1 using the BIAcore biosensor. After the second panning, supernatants of *E. coli* TG1 included phagemid were randomly collected and performed the screening by ELISA and bioassay to analyze their bioactivity and affinity against TNFR1 (*data not shown*). As a result, we identified six TNFR1-selective, high affinity clones, R1-15 to R1-20 (Table 1). Similarly, we identified three TNFR2-selective candidates (R2-14 to R2-16) from the Shuffling Library B (Table 1). The fact that the amino acid residue at position 87 in all active TNF receptor-selective candidates was a Tyr residue (Table 1), it suggests that Tyr87 is an important residues

Table 1
Substituted residues and affinities of TNF receptor-selective mutant candidates.

	Amino acid sequence												Relative affinity (%)[a]		
	29	31	32	84	85	86	87	88	89	145	146	147	TNFR1	TNFR2	TNFR1/TNFR2
wtTNF	L	R	R	A	V	S	Y	Q	T	A	E	S	100.0	100.0	1.0
R1-5[b]	K	A	G	–	–	–	–	–	–	–	S	T	82.0	2.0×10^{-2}	4.1×10^3
R1-15	R	N	Y	S	–	R	–	N	P	–	–	–	115.7	6.0×10^{-2}	1.9×10^3
R1-16	T	Q	Y	T	P	G	–	S	H	–	A	H	8.6	6.0×10^{-2}	1.4×10^2
R1-17	R	T	F	S	P	L	–	R	Q	S	S	T	54.2	6.0×10^{-2}	9.0×10^2
R1-18	K	N	F	S	S	H	–	T	H	–	–	–	53.9	1.0×10^{-1}	5.4×10^2
R1-19	S	N	Y	–	–	–	–	–	–	–	V	–	138.7	8.0×10^{-1}	1.7×10^3
R1-20	T	–	Y	S	H	T	–	P	S	S	Q	A	170.5	3.0×10^{-2}	5.7×10^3
R2-3[c]	–	–	–	–	–	–	–	–	–	R	–	T	<0.1	33.4	<0.0029
R2-14	–	–	–	–	P	–	–	N	S	S	A	D	1.6	103.7	0.0154
R2-15	–	–	–	S	Q	A	–	N	–	I	G	D	<0.1	141.8	<0.0007
R2-16	–	–	–	–	–	–	–	–	–	H	S	D	1.4	91.7	0.0152

Comparison of the amino acid residues of the wild-type and mutant TNFs; conserved residues are indicated using a dash.

[a] Concentration of mutant TNF required for 50% inhibition of maximal binding of wtTNF-FLAG.

[b] A TNFR1-selective mutant, which was isolated previously from the existing phage library (Library I).

[c] A TNFR2-selective mutant, which was isolated obtained from the existing phage library (Library I).

for receptor binding, which is in good agreement with the previous report [8–10].

To determine the properties of the receptor-selective candidates, we purified all the candidate TNF mutants as recombinant proteins using a general recombinant protein technology [11,12,15,18]. After each recombinant mutant TNF was expressed in *E. coli* BL21λDE3 and purified to homogeneity, we used gel electrophoresis and gel filtration chromatography to confirm that each of them, like the wtTNF, displayed MW of 17 kDa and formed a homotrimeric complex (*results not shown*). We next used a competitive ELISA to examine the binding properties of the mutant TNFs to the TNF receptors, and the results are summarized in Table 1. As summarized, all TNFR1-selective candidates showed lower affinity for TNFR2 than the wtTNF. On the other hand, affinities of the clones R1-15, R1-19, and R1-20 for TNFR1 were better than that the wtTNF. Especially, affinity of the clone R1-20 for TNFR1 was more than 1.7-fold higher than that of the wtTNF and was about 2-fold higher than that of the TNF mutant R1-5, which was previously identified from the Library I [12]. Additionally, selectivity of R1-20 for TNFR1 was higher than that of the R1-5. Next, we evaluated affinity of the TNFR2-selective mutants for TNFR2 (Table 1). Our results revealed that the clones R2-14, R2-15 and R2-16 bound to TNFR2 more strongly than the TNF mutant R2-3, which was previously isolated in our laboratory [12]. Especially, the TNF mutant R2-15 bound to TNFR2 with an affinity that was 1.4-fold higher than that of the wtTNF. R2-15 also showed superior TNFR2-selectivity than R2-3. Thus, by using the gene shuffling libraries, we were able to isolate TNF mutants that were highly receptor-selective. The receptor-selective TNF mutants R1-20 and R2-15 contained amino acid substitutions at 10 and 7 places, respectively. A point mutation analysis study of TNF suggested that the amino acid residues near position 140 are essential for TNFR1 binding [8,10,12]. In agreement with this report, we found that the residue at position 145 in the TNFR1-specific mutants is mostly retained or contained conservative amino acid substitutions, whereas more than one residues at positions 145, 146 and 147 in the TNFR2-selective mutants contained non-conservative amino acid substitutions. On the other hand, the amino acids residues near positions 30 and 80 were mostly conserved in the TNFR2-specific mutants, but not in the TNFR1-specifc mutants, suggesting that these amino acid residues might play important roles in TNFR2 binding [12]. Thus, this is the first report describing the creation of highly receptor-selective TNF mutants, namely R1-20 and R2-15, from a randomized mutant TNF library containing amino acid substitutions at 12 different amino acid residues. These results clearly demonstrate the usefulness of the developed method, which combines both phage display and gene shuffling techniques.

Next, we examined the receptor-selective bioactivities of the TNF mutants R1-20 and R2-15, each one of which showed highest receptor-selectivity, and the results are shown in Fig. 2 and Table 2. TNFR1-mediated cytotoxicity induced by the TNF mutant R1-20, as measured *in vitro* using the Hep-2 cells, was 7-fold and 2.2-fold higher than those of the mutant R1-5 and wtTNF, respectively (Fig. 2A and Table 2). Next, we evaluated the TNFR2-mediated activity of R1-20 using the hTNFR2/mFas-preadipocyte cells, which were previously constructed in our laboratory [14]. As expected, R1-20 hardly exhibited bioactivity via TNFR2, and the activity was much lower than that of the wtTNF (Fig. 2B and Table 2). On the other hand, the bioactivity of the TNFR2-selective mutant R2-15 via TNFR1 was 1000-fold lower than that of the wtTNF (Fig. 2C). The bioactivity of R2-15 via TNFR2 was, however, 2.5-fold higher than that of the wtTNF and more than 15-fold higher than that of the R2-3 mutant (Fig. 2D and Table 2). Remarkably, the bioactivity of R2-15 was higher that that of the R2-3, both of which are TNFR2-specific TNF mutants (Fig. 2D and Table 2).

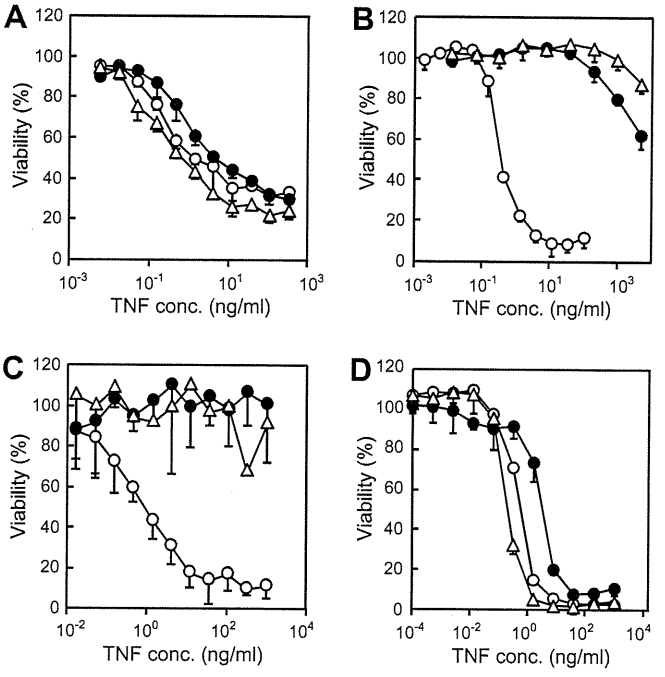

Fig. 2. Bioactivity of the receptor-selective mutants. The receptor-specific bioactivity (% viability) was measured following the treatment of HEp-2 or hTNFR2/mFas-preadipocyte cells with the wild-type or mutant TNF by using the methylene blue staining procedure as described in Materials and methods. (A) and (C) TNFR1-mediated bioactivity was measured using the HEp-2 cells. (B) and (D) TNFR2-mediated bioactivity was measured using the hTNFR2/mFas-preadipocyte cells. In (A) and (B) open circle, wtTNF; closed circle, R1-5; and open triangle, R1-20. In (C) and (D) open circle, wtTNF; closed circle, R2-3; and open triangle, R2-15.

Table 2
Bioactivity of receptor-selective mutants.

	TNFR1[a]		TNFR2[b]	
	EC50 (ng/ml)	Relative (%)	EC50 (ng/ml)	Relative (%)
wtTNF	1.3	100.0	0.4	100.0
R1-5	4.4	29.5	$>5.0 \times 10^5$	$<8.0 \times 10^{-5}$
R1-20	0.6	216.7	$>5.0 \times 10^5$	$<8.0 \times 10^{-5}$
R2-3	$>1.0 \times 10^3$	<0.1	3.1	13.0
R2-15	$>1.0 \times 10^3$	<0.1	0.2	200.0

The bioactivity values were determined from the results shown in Fig. 2 and are shown here as relative values (% wtTNF). Each value shown is mean ± SD ($n = 3$).

[a] TNFR1-mediated bioactivity was determined by a cytotoxicity assay as described in Materials and methods using the HEp-2 cells.

[b] TNFR2-mediated bioactivity was determined by a cytotoxicity assay as described in Materials and methods using the hTNFR2/mFas-preadipocyte cells.

Thus, by using the combined technology described in this study, we were able to identify TNF mutants with improved TNF receptor-selectivity and enhanced bioactivity than the existing TNF mutants.

Presently, both the underlying mechanism of signal transduction via each TNF receptor, and the relationship between the TNF receptors and onset of TNF-related diseases remain unclear. We anticipate that the TNF receptor-selective TNF mutants found in this study could be used as tools to analyze the receptor-specific signal transduction pathways. Additionally, we believe that the technology described here would be easily applicable to many disease-related proteins of unknown function. Thus, by creating structurally diverse protein libraries, we could rapidly identify therapeutically valuable proteins, which might lead to the development of effective and safe drugs in the near future.

Acknowledgments

This study was supported in part by Grants-in-Aid for Scientific Research from the Ministry of Education, Culture, Sports, Science and Technology of Japan, and by Grants-in-Aid for Scientific Research from Japan Society for the Promotion of Science (JSPS). In addition, this study was also supported in part by Health Labour Sciences Research Grants from the Ministry of Health, Labor and Welfare of Japan, Health Sciences Research Grants for Research on Publicly Essential Drugs and Medical Devices from the Japan Health Sciences Foundation, as well as The Nagai Foundation Tokyo.

References

[1] H. Wajant, K. Pfizenmaier, P. Scheurich, Tumor necrosis factor signaling, Cell Death Differ. 10 (2003) 45–65.
[2] Y. Muto, K.T. Nouri-Aria, A. Meager, G.J. Alexander, A.L. Eddleston, R. Williams, Enhanced tumour necrosis factor and interleukin-1 in fulminant hepatic failure, Lancet 2 (1988) 72–74.
[3] M. Feldmann, R.N. Maini, Lasker Clinical Medical Research Award. TNF defined as a therapeutic target for rheumatoid arthritis and other autoimmune diseases, Nat. Med. 9 (2003) 1245–1250.
[4] J. Keane, S. Gershon, R.P. Wise, E. Mirabile-Levens, J. Kasznica, W.D. Schwieterman, J.N. Siegel, M.M. Braun, Tuberculosis associated with infliximab, a tumor necrosis factor alpha-neutralizing agent, N. Engl. J. Med. 345 (2001) 1098–1104.
[5] N. Shakoor, M. Michalska, C.A. Harris, J.A. Block, Drug-induced systemic lupus erythematosus associated with etanercept therapy, Lancet 359 (2002) 579–580.
[6] T. Weiss, M. Grell, K. Siemienski, F. Muhlenbeck, H. Durkop, K. Pfizenmaier, P. Scheurich, H. Wajant, TNFR80-dependent enhancement of TNFR60-induced cell death is mediated by TNFR-associated factor 2 and is specific for TNFR60, J. Immunol. 161 (1998) 3136–3142.
[7] M. Fotin-Mleczek, F. Henkler, D. Samel, M. Reichwein, A. Hausser, I. Parmryd, P. Scheurich, J.A. Schmid, H. Wajant, Apoptotic crosstalk of TNF receptors: TNF-R2-induces depletion of TRAF2 and IAP proteins and accelerates TNF-R1-dependent activation of caspase-8, J. Cell Sci. 115 (2002) 2757–2770.
[8] X. Van Ostade, J. Tavernier, W. Fiers, Structure–activity studies of human tumour necrosis factors, Protein Eng. 7 (1994) 5–22.
[9] X.M. Zhang, I. Weber, M.J. Chen, Site-directed mutational analysis of human tumor necrosis factor-alpha receptor binding site and structure–functional relationship, J. Biol. Chem. 267 (1992) 24069–24075.
[10] J. Yamagishi, H. Kawashima, N. Matsuo, M. Ohue, M. Yamayoshi, T. Fukui, H. Kotani, R. Furuta, K. Nakano, M. Yamada, Mutational analysis of structure–activity relationships in human tumor necrosis factor-alpha, Protein Eng. 3 (1990) 713–719.
[11] H. Shibata, Y. Yoshioka, A. Ohkawa, K. Minowa, Y. Mukai, Y. Abe, M. Taniai, T. Nomura, H. Kayamuro, H. Nabeshi, T. Sugita, S. Imai, K. Nagano, T. Yoshikawa, T. Fujita, S. Nakagawa, A. Yamamoto, T. Ohta, T. Hayakawa, T. Mayumi, P. Vandenabeele, B.B. Aggarwal, T. Nakamura, Y. Yamagata, S. Tsunoda, H. Kamada, Y. Tsutsumi, Creation and X-ray structure analysis of the tumor necrosis factor receptor-1-selective mutant of a tumor necrosis factor-alpha antagonist, J. Biol. Chem. 283 (2008) 998–1007.
[12] Y. Mukai, H. Shibata, T. Nakamura, Y. Yoshioka, Y. Abe, T. Nomura, M. Taniai, T. Ohta, S. Ikemizu, S. Nakagawa, S. Tsunoda, H. Kamada, Y. Yamagata, Y. Tsutsumi, Structure–function relationship of tumor necrosis factor (TNF) and its receptor interaction based on 3D structural analysis of a fully active TNFR1-selective TNF mutant, J. Mol. Biol. 385 (2009) 1221–1229.
[13] H. Shibata, Y. Yoshioka, A. Ohkawa, Y. Abe, T. Nomura, Y. Mukai, S. Nakagawa, M. Taniai, T. Ohta, T. Mayumi, H. Kamada, S. Tsunoda, Y. Tsutsumi, The therapeutic effect of TNFR1-selective antagonistic mutant TNF-α in murine hepatitis models, Cytokine 44 (2008) 229–233.
[14] Y. Abe, T. Yoshikawa, H. Kamada, H. Shibata, T. Nomura, K. Minowa, H. Kayamuro, K. Katayama, H. Miyoshi, Y. Mukai, Y. Yoshioka, S. Nakagawa, S. Tsunoda, Y. Tsutsumi, Simple and highly sensitive assay system for TNFR2-mediated soluble- and transmembrane-TNF activity, J. Immunol. Methods 335 (2008) 71–78.
[15] Y. Yamamoto, Y. Tsutsumi, Y. Yoshioka, T. Nishibata, K. Kobayashi, T. Okamoto, Y. Mukai, T. Shimizu, S. Nakagawa, S. Nagata, T. Mayumi, Site-specific PEGylation of a lysine-deficient TNF-alpha with full bioactivity, Nat. Biotechnol. 21 (2003) 546–552.
[16] C.R. Brunetti, M. Paulose-Murphy, R. Singh, J. Qin, J.W. Barrett, A. Tardivel, P. Schneider, K. Essani, G. McFadden, A secreted high-affinity inhibitor of human TNF from Tanapox virus, Proc. Natl. Acad. Sci. USA 100 (2003) 4831–4836.
[17] Y. Tsutsumi, T. Kihira, S. Tsunoda, T. Kanamori, S. Nakagawa, T. Mayumi, Molecular design of hybrid tumour necrosis factor alpha with polyethylene glycol increases its anti-tumour potency, Br. J. Cancer 71 (1995) 963–968.
[18] H. Shibata, Y. Yoshioka, S. Ikemizu, K. Kobayashi, Y. Yamamoto, Y. Mukai, T. Okamoto, M. Taniai, M. Kawamura, Y. Abe, S. Nakagawa, T. Hayakawa, S. Nagata, Y. Yamagata, T. Mayumi, H. Kamada, Y. Tsutsumi, Functionalization of tumor necrosis factor-alpha using phage display technique and PEGylation improves its antitumor therapeutic window, Clin. Cancer Res. 10 (2004) 8293–8300.

National Institute of Biomedical Innovation (NiBio)[1]; Graduate School of Pharmaceutical Sciences[2], Osaka University; The Center for Advanced Medical Engineering and Informatics[3], Osaka University, Osaka, Japan

Creation of an improved mutant TNF with TNFR1-selectivity and antagonistic activity by phage display technology

T. NOMURA[1,2*], Y. ABE[1*], H. KAMADA[1,3], M. INOUE[1], T. KAWARA[1,2], S. ARITA[1,2], T. FURUYA[1,2], K. MINOWA[1], Y. YOSHIOKA[2,3], H. SHIBATA[1], H. KAYAMURO[1,2], T. YAMASHITA[1,2], K. NAGANO[1], T. YOSHIKAWA[1,2], Y. MUKAI[2], S. NAKAGAWA[2,3], S. TSUNODA[1,2,3], Y. TSUTSUMI[1,2,3]

Received August 7, 2009, accepted August 14, 2009

Shin-ichi Tsunoda, Ph.D., Laboratory of Pharmaceutical Proteomics, National Institute of Biomedical Innovation, 7-6-8 Saito-Asagi, Ibaraki, Osaka 567-0085, Japan
tsunoda@nibio.go.jp
**These authors contributed equally to the work.*

Pharmazie 65: 93–96 (2010) *doi: 10.1691/ph.2010.9265*

Tumor necrosis factor-α (TNF), which binds two types of TNF receptors (TNFR1 and TNFR2), regulates the onset and exacerbation of autoimmune diseases such as rheumatoid arthritis and Crohn's disease. In particular, TNFR1-mediated signals are predominantly related to the induction of inflammatory responses. We have previously generated a TNFR1-selective antagonistic TNF-mutant (mutTNF) and shown that mutTNF efficiently inhibits TNFR1-mediated bioactivity *in vitro* and attenuates inflammatory conditions *in vivo*. In this study, we aimed to improve the TNFR1-selectivity of mutTNF. This was achieved by constructing a phage library displaying mutTNF-based variants, in which the amino acid residues at the predicted receptor binding sites were substituted to other amino acids. From this mutant TNF library, 20 candidate TNFR1-selective antagonists were isolated. Like mutTNF, all 20 candidates were found to have an inhibitory effect on TNFR1-mediated bioactivity. However, one of the mutants, N7, displayed significantly more than 40-fold greater TNFR1-selectivty than mutTNF. Therefore, N7 could be a promising anti-autoimmune agent that does not interfere with TNFR2-mediated signaling pathways.

1. Introduction

The severity and progression of inflammatory diseases, such as rheumatoid arthritis, Crohn's disease and ulcerative colitis, can be correlated with the serum level of tumor necrosis factor-α (TNF). Thus, TNF blockades such as anti-TNF antibodies and soluble TNFRs, which neutralize the activity of TNF, have been used to treat various autoimmune diseases in clinical practice. However, TNF blockades inhibit both TNFR1 and TNFR2 signaling. Thus, treatment with these drugs can lead to an increased risk of infection (Gomez-Reino et al. 2003; Lubel et al. 2007) and lymphoma development (Brown et al. 2002). TNF has been reported to induce inflammatory response predominantly through TNFR1 (Mori et al. 1996), whereas activation of the immune response is initiated *via* TNFR2 (Kim et al. 2006; Kim and Teh 2001; Grell et al. 1998). Therefore, blocking TNFR1-signaling, but not TNFR2-signaling, is a promising strategy for the safe and effective treatment of inflammatory diseases, which overcomes the risk of infection associated with the use of non-specific TNF blockades (Kollias and Kontoyiannis 2002).
In our previous studies, we used the phage display technique (Imai et al. 2008; Nagano et al. 2009; Nomura et al. 2007) to generate a TNFR1-selective antagonistic mutant TNF (mutTNF) that blocks TNFR1-mediated signals but not those of TNFR2 (Shibata et al. 2008b). Moreover, mutTNF showed superior therapeutic effects using an inflammatory disease mouse model (Shibata et al. 2008a). Thus, a drug for autoimmune diseases that selectively targets TNFR1 is anticipated to display higher efficacy and safety compared to existing treatments. In this study, we have attempted to isolate TNFR1-selective antagonists with higher TNFR1-selectivity than previous mutTNF by constructing a modified phage library displaying mutTNF-based variants.

2. Investigations, results and discussion

Here, we attempted to improve the TNFR1-selectivity of mutTNF using a phage display technique. Firstly, we constructed a phage library of TNF mutant using mutTNF as template. We designed a randomized library of mutTNF to replace the six amino acid residues (aa 29, 31, 32, 145–147) in the predicted receptor binding site. As a result of the 2-step PCR, we confirmed that the mutTNF mutant library consisted of 4×10^7 independent recombinant clones (*data not shown*). To enrich for TNFR1-selective antagonists, the phage library was subjected to two rounds of panning against TNFR1 on a Biacore biosensor chip. After the second panning, supernatants of single clone of *E. coli* TG1 including phagemid were randomly collected and subjected to screening by bioassay and ELISA to evaluate their bioactivity and affinity against each TNF receptor, respectively (*data not shown*). Consequently, twenty candidates of TNFR1-selective mutants with antagonistic activity were isolated (Table).
Next, we determined the detailed biological properties of each candidate. Positive clones were engineered for expression in

Table: Amino acid sequences and biological properties of TNFR1-selective antagonist candidates

TNF	Amino acid sequence						Relative affinity (% K_d)[a]			Bioactivity via TNFR1	
	29	31	32	145	146	147	TNFR1	TNFR2	TNFR1[b]/TNCR2	Agonistic[c] activity	Antagonisti[d] activity
mutTNF	L	R	R	A	E	S	100.0	100.0	1.0	–	+
N1	S	–	W	R	–	–	550.0	21.6	25.5	+	–
N2	S	–	W	–	–	–	200.0	N.D.	N.D.	+	–
N3	S	–	W	R	D	–	550.0	44.8	12.3	–	±
N4	S	–	W	–	D	–	183.3	19.1	9.6	±	–
N5	S	–	W	–	S	E	275.0	25.8	10.7	±	–
N6	A	D	T	–	–	–	200.0	21.6	9.3	±	–
N7	S	N	D	D	A	–	104.7	2.5	41.9	–	+
N8	R	I	A	D	–	–	169.2	26.7	6.3	+	–
N9	H	H	–	–	N	G	169.2	33.0	5.1	+	–
N10	T	N	N	–	–	–	314.3	28.6	11.0	±	–
N11	T	N	N	S	–	–	275.0	18.3	15.0	±	–
N12	F	S	T	–	–	–	440.0	58.0	7.6	+	–
N13	F	S	T	–	S	E	440.0	73.9	6.0	+	–
N14	R	W	Y	T	N	T	314.3	19.2	16.4	+	–
N15	F	K	T	N	A	T	275.0	24.1	11.4	±	–
N16	M	L	T	N	S	T	367.0	7.7	47.7	+	–
N17	Y	L	A	T	H	T	137.5	1.6	86.0	±	–
N18	Y	L	A	T	H	–	110.0	4.7	23.4	±	–
N19	V	Q	Y	N	N	–	367.0	N.D.	N.D.	±	–
N20	F	S	T	P	Q	R	244.4	N.D.	N.D.	±	–

Conserved residues compared with mutTNF are indicated by an em dash (–) The affinity values are shown as relative values (% mutTNF). N.D.: not detected

[a] Affinity for immobilized TNFR1 and TNFR2 was assessed by SPR using BIAcore3000. The dissociation constant (K_d) of TNF mutants were calculated from their sensorgrams by BIAEVALUATION 4.0 software

[b] TNFR1-selectivity was defined as relative affinity [TNFE1]/ relative affinity [TNFR2] for mutTNF

[c] TNFR1-mediated agonistic activity was measured, using a HEp-2 cell cytotoxicity assay. The intensity in agonistic activity was evaluated as the following. Cell viability at 10^4 ng/ml each mutant. 0–25% (of non treatment); (+), 25–50%; (±), 50–100%; (–)

[d] TNFR1-mediated antagonistic activity of mutant TNFs on wtTNF induced cytotoxicity in HEp-2 cells was measured. The intensity in antagonistic activity was evaluated as the following. Cell viability at 10^5 ng/ml each mutant in present of 5 ng/ml wtTNF. 0–25% (of non treatment); (–), 25–50%; (±), 50–100%; (+)

E. coli BL21λDE3 and each recombinant protein was purified as described previously (Yamamoto 2003). As anticipated, gel electrophoresis confirmed the mutant TNF proteins to have a molecular weight of 17 kDa. Moreover, gel filtration chromatography established that each mutant forms a homotrimeric complex in solution, as is the case for wild-type TNF (wtTNF) (*data not shown*). To analyze the binding properties of these TNFR1-selective TNF candidates, their dissociation constants (K_d) for TNFR1 and TNFR2 were measured using a surface plasmon resonance (SPR) analyzer. Our previous SPR analysis showed that although mutTNF has an almost identical affinity to TNFR1 as to wtTNF, it displays more than 17,000-fold greater selectivity for TNFR1. As shown in the Table, all the candidates exhibited higher affinity for TNFR1 than mutTNF. Furthermore, clones N1, N7, N16, N17 and N18 showed more than 20-fold higher TNFR1-binding selectivity compared to mutTNF. To examine the bioactivity of all candidates *via* TNFR1, we subsequently performed a cytotoxicity assay using

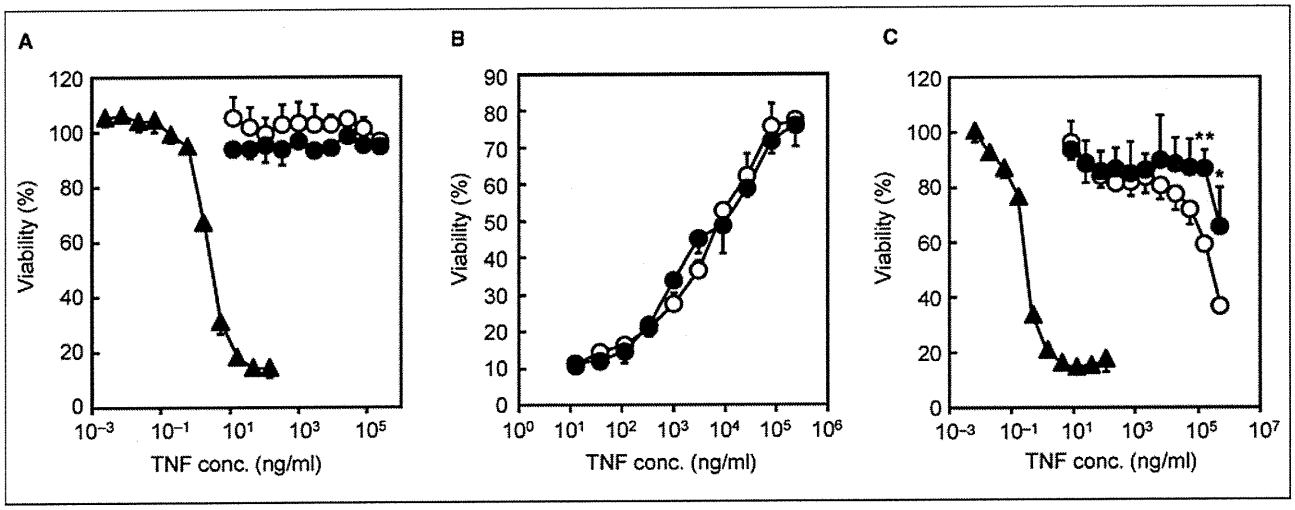

Fig.: Bioactivities and antagonistic activities of N7. (A) To determine the TNFR1-mediated bioactivities, several dilutions of wtTNF (closed triangle), mutTNF (open circle) and N7 (closed circle) were added to L-M cells and incubated for 4 h at 37 °C. (B) Indicated dilutions of mutTNF (open circle) and N7 (closed circle) and constant of wtTNF (5 ng/ml) were mixed and added to L-M cells and incubated for 4 h at 37 °C. TNFR1-mediated antagonistic activity was assessed as described in the Experimental section. (C) To determine the TNFR2-mediated bioactivities, diluted wtTNF (closed triangle), mutTNF (open circle) and N7 (closed circle) were added to hTNFR2/mFas-preadipocyte cells and incubated for 48 h at 37 °C. After incubation, cell viability was measured using the methylene blue assay. Data represent the mean ± S.D. and were analyzed by Student's t-test (*$p < 0,05$, **$p < 0,01$ vs mutTNF)

HEp-2 cells (Table). As anticipated, mutTNF was unable to activate TNFR1. Likewise clones N3 and N7 do not activate TNFR1 signaling, even when tested at high concentrations. The TNFR1-mediated antagonistic assay demonstrated that N7 showed the highest activity of all the TNFR1-selective antagonist candidates. The Figure show details of bioactivities and antagonistic activities of N7. The TNFR1-mediated agonistic activity using L-M cells showed that wtTNF displays TNFR1-mediated agonistic activity in a dose-dependent manner. In contrast, N7, in addition to mutTNF, barely displays any agonistic activity (Fig. A). Moreover, N7 had an almost identical antagonistic activity for TNFR1-mediated bioactivity to that of mutTNF (Fig. B). Next, TNFR2-mediated activities of these TNFR1-selective antagonists were measured using hTNFR2/mFas-preadipocyte cells. The bioactivity of mutTNF and N7 *via* TNFR2 was much lower than that of wtTNF. Remarkably, TNFR2-mediated agonistic activity of N7 was lower than that of mutTNF, in agreement with the reduced affinity for TNFR2 (Fig. C).

In conclusion, we have succeeded in creating a TNFR1-selective antagonist with improved TNFR1-selectivity over that of mutTNF. This was achieved by constructing a library of mutTNF variants using a phage display technique. While TNFR1 is believed to be important for immunological responses (Rothe et al. 1993), TNFR2 is thought to be important for antiviral resistance and is effective for controlling mycobacterial infection by affecting membrane-bound TNF stimulation (Saunders et al. 2005; Olleros et al. 2002). Therefore, use of N7 might reduce the risk of side effects, such as infections, when applying TNF blockade as a therapy for autoimmune disease. We are currently evaluating the therapeutic effect of N7 using a mouse autoimmune disease model.

3. Experimental

3.1. Cell culture

HEp-2 cells (a human fibroblast cell line) were provided by Cell Resource Center for Biomedical Research (Tohoku University, Sendai) and were maintained in RPMI 1640 medium supplemented with 10% FBS and 1% antibiotics cocktail (penicillin 10,000 units/ml, streptomycin 10 mg/ml, and amphotericin B 25 μg/ml). L-M cells (a mouse fibroblast cell line) were provided by Mochida Pharmaceutical Co. Ltd. (Tokyo, Japan) and were maintained in minimum Eagle's medium supplemented with 1% FBS and 1% antibiotics cocktail. hTNFR2/mFas-preadipocyte cells were established previously in our laboratory (Abe et al. 2008) and were maintained in Dulbecco's modified Eagle's medium supplemented with Blasticidin S HCl, 10% FBS, 1 mM sodium pyruvate, 5×10^{-5} M 2-mercaptoethanol, and 1% antibiotic cocktail.

3.2. Construction of a novel gene library displaying mutTNF variants

The pCANTAB phagemid vector encoding mutTNF was used as template for PCR. The mutTNF was created in previous study and showed TNFR1-selective antagonistic activity (Shibata et al. 2008b). The six amino acid residues at the receptor binding site (amino acid residues; 29, 31, 32 and 145–147) of mutTNF were replaced with other amino acids using a 2-step PCR procedure as described previously (Mukai et al. 2009).

3.3. Selection of TNFR1-selective antagonist candidates from a mutTNF mutated phage library

Human TNFR1 Fc chimera (R&D systems, Minneapolis, MN) was immobilized onto a CM3 sensor chip as described previously. Briefly, the phage display library (1×10^{11} CFU/100 μl) was injected over the sensor chip at a flow rate of 3 μl/min. After binding, the sensor chip was washed using the rinse command until the association phase was reached. Elution was carried out using 4 μl of 10 mM glycine-HCl. The eluted phage pool was neutralized with 1 M Tris-HCl (pH 6.9) and then used to infect *E. coli* TG1 in order to amplify the phage. The panning steps were repeated twice. Subsequently, single clones were isolated and supernatant from each clone was collected and used to determine the cytotoxicity in the HEp-2 cytotoxic assay and the affinity for TNFR1 by ELISA, respectively (Shibata et al. 2008b). We screened clones having almost no cytotoxicity but significant affinity for TNFR1. The phagemids purified from single clones were sequenced using the Big Dye Terminator v3.1 kit (Applied Biosystems, Foster City, CA). Sequencing reactions were analyzed on an ABI PRISM 3100 (Applied Biosystems).

3.4. Surface plasmon resonance assay (BIAcore® assay)

The binding kinetics of the proteins were analyzed by the surface plasmon resonance technique by BIAcore® (GE Healthcare, Amersham, UK). Each TNF receptor was immobilized onto a CM5 sensor chip, which resulted in an increase of 3,000–3,500 resonance units. During the association phase, all clones serially diluted in running buffer (HBS-EP) were allowed to pass over TNFR1 and TNFR2 at a flow rate of 20 μl/min. Kinetic parameters for each candidate were calculated from the respective sensorgram using BIAevaluation 4.0 software.

3.5. Cytotoxicity assay

In order to measure TNFR1-mediated cytotoxicity, HEp-2 or L-M cells were cultured in 96-well plates in the presence of TNF mutants and serially diluted wtTNF (Peprotech, Rocky Hill, NJ) with 100 μg/ml cycloheximide for 18 h at 4×10^4 cells/well or for 48 h at 1×104 cells/well. Cytotoxicity was then assessed using the methylene blue assay as described previously (Mukai et al. 2009; Shibata et al. 2004). For the TNFR1-mediated antagonistic assay, cells were cultured in the presence of 5 ng/ml human wtTNF and a serial dilution of the mutTNF. For the TNFR2-mediated cytotoxic assay, hTNFR2/mFas-preadipocyte cells were cultured in 96-well plates in the presence of TNF mutants and serially diluted wtTNF (1×10^4 cells/well) (Abe et al. 2008). After incubation for 48 h, cell survival was determined using the methylene blue assay.

Acknowledgement: This study was supported in part by Grants-in-Aid for Scientific Research from the Ministry of Education, Culture, Sports, Science and Technology of Japan, and by Grants-in-Aid for Scientific Research from Japan Society for the Promotion of Science (JSPS). In addition, this study was also supported in part by Health Labour Sciences Research Grants from the Ministry of Health, Labor and Welfare of Japan, Health Sciences Research Grants for Research on Publicly Essential Drugs and Medical Devices from the Japan Health Sciences Foundation and by a Grant from the Minister of the Environment, as well as THE NAGAI FOUNDATION TOKYO.

References

Abe Y, Yoshikawa T, Kamada H, Shibata H, Nomura T, Minowa K, Kayamuro H, Katayama K, Miyoshi H, Mukai Y, Yoshioka Y, Nakagawa S, Tsunoda S, Tsutsumi Y (2008) Simple and highly sensitive assay system for TNFR2-mediated soluble- and transmembrane-TNF activity. J Immunol Methods 335: 71–78.

Aggarwal BB (2003) Signalling pathways of the TNF superfamily: a double-edged sword. Nat Rev Immunol 3: 745–756.

Brown SL, Greene MH, Gershon SK, Edwards ET, Braun MM (2002) Tumor necrosis factor antagonist therapy and lymphoma development: twenty-six cases reported to the Food and Drug Administration. Arthritis Rheum 46: 3151–3158.

Feldmann M (2002) Development of anti-TNF therapy for rheumatoid arthritis. Nat Rev Immunol 2: 364–371.

Goldbach-Mansky R, Lipsky PE (2003) New concepts in the treatment of rheumatoid arthritis. Annu Rev Med 54: 197–216.

Gomez-Reino JJ, Carmona L, Valverde VR, Mola EM, Montero MD (2003) Treatment of rheumatoid arthritis with tumor necrosis factor inhibitors may predispose to significant increase in tuberculosis risk: a multicenter active-surveillance report. Arthritis Rheum 48: 2122–2127.

Grell M, Becke FM, Wajant H, Mannel DN, Scheurich P (1998) TNF receptor type 2 mediates thymocyte proliferation independently of TNF receptor type 1. Eur J Immunol 28: 257–263.

Imai S, Mukai Y, Takeda T, Abe Y, Nagano K, Kamada H, Nakagawa S, Tsunoda S, Tsutsumi Y (2008) Effect of protein properties on display efficiency using the M13 phage display system. Pharmazie 63: 760–764.

Kim EY, Priatel JJ, Teh SJ, Teh HS (2006) TNF receptor type 2 (p75) functions as a costimulator for antigen-driven T cell responses *in vivo*. J Immunol 176: 1026–1035.

Kim EY, Teh HS (2001) TNF type 2 receptor (p75) lowers the threshold of T cell activation. J Immunol 167: 6812–6820.

Kollias G, Kontoyiannis D (2002) Role of TNF/TNFR in autoimmunity: specific TNF receptor blockade may be advantageous to anti-TNF treatments. Cytokine Growth Factor Rev 13: 315–321.

Lubel JS, Testro AG, Angus PW (2007) Hepatitis B virus reactivation following immunosuppressive therapy: guidelines for prevention and management. Intern Med J 37: 705–712.

Mori L, Iselin S, De Libero G, Lesslauer W (1996) Attenuation of collagen-induced arthritis in 55-kDa TNF receptor type 1 (TNFR1)-IgG1-treated and TNFR1-deficient mice. J Immunol 157: 3178–3182.

Mukai Y, Shibata H, Nakamura T, Yoshioka Y, Abe Y, Nomura T, Taniai M, Ohta T, Ikemizu S, Nakagawa S, Tsunoda S, Kamada H, Yamagata Y, Tsutsumi Y (2009) Structure-function relationship of tumor necrosis factor (TNF) and its receptor interaction based on 3D structural analysis of a fully active TNFR1-selective TNF mutant. J Mol Biol 385: 1221–1229.

Nagano K, Imai S, Mukai Y, Nakagawa S, Abe Y, Kamada H, Tsunoda S, Tsutsumi Y (2009) Rapid isolation of intrabody candidates by using an optimized non-immune phage antibody library. Pharmazie 64: 238–241.

Nomura T, Kawamura M, Shibata H, Abe Y, Ohkawa A, Mukai Y, Sugita T, Imai S, Nagano K, Okamoto T, Tsutsumi Y, Kamada H, Nakagawa S, Tsunoda S (2007) Creation of a novel cell penetrating peptide, using a random 18mer peptides library. Pharmazie 62: 569–573.

Olleros ML, Guler R, Corazza N, Vesin D, Eugster HP, Marchal G, Chavarot P, Mueller C, Garcia I (2002) Transmembrane TNF induces an efficient cell-mediated immunity and resistance to Mycobacterium bovis bacillus Calmette-Guerin infection in the absence of secreted TNF and lymphotoxin-alpha. J Immunol 168: 3394–3401.

Rothe J, Lesslauer W, Lotscher H, Lang Y, Koebel P, Kontgen F, Althage A, Zinkernagel R, Steinmetz M, Bluethmann H (1993) Mice lacking the tumour necrosis factor receptor 1 are resistant to TNF-mediated toxicity but highly susceptible to infection by Listeria monocytogenes. Nature 364: 798–802.

Saunders BM, Tran S, Ruuls S, Sedgwick JD, Briscoe H, Britton WJ (2005) Transmembrane TNF is sufficient to initiate cell migration and granuloma formation and provide acute, but not long-term, control of Mycobacterium tuberculosis infection. J Immunol 174: 4852–4859.

Shibata H, Yoshioka Y, Ikemizu S, Kobayashi K, Yamamoto Y, Mukai Y, Okamoto T, Taniai M, Kawamura M, Abe Y, Nakagawa S, Hayakawa T, Nagata S, Yamagata Y, Mayumi T, Kamada H, Tsutsumi Y (2004) Functionalization of tumor necrosis factor-alpha using phage display technique and PEGylation improves its antitumor therapeutic window. Clin Cancer Res 10: 8293–8300.

Shibata H, Yoshioka Y, Ohkawa A, Abe Y, Nomura T, Mukai Y, Nakagawa S, Taniai M, Ohta T, Mayumi T, Kamada H, Tsunoda S, Tsutsumi Y (2008a) The therapeutic effect of TNFR1-selective antagonistic mutant TNF-alpha in murine hepatitis models. Cytokine 44: 229–233.

Shibata H, Yoshioka Y, Ohkawa A, Minowa K, Mukai Y, Abe Y, Taniai M, Nomura T, Kayamuro H, Nabeshi H, Sugita T, Imai S, Nagano K, Yoshikawa T, Fujita T, Nakagawa S, Yamamoto A, Ohta T, Hayakawa T, Mayumi T, Vandenabeele P, Aggarwal BB, Nakamura T, Yamagata Y, Tsunoda S, Kamada H, Tsutsumi Y (2008b) Creation and X-ray structure analysis of the tumor necrosis factor receptor-1-selective mutant of a tumor necrosis factor-alpha antagonist. J Biol Chem 283: 998–1007.

Yamamoto Y, Tsutsumi Y, Yoshioka Y, Nishibata T, Kobayashi K, Okamoto T, Mukai Y, Shimizu T, Nakagawa S, Nagata S, Mayumi T (2003) Site-specific PEGylation of a lysine-deficient TNF-alpha with full bioactivity. Nat Biotechnol 21: 546–552.

OPEN ACCESS Freely available online

PLoS one

A Novel Screening System for Claudin Binder Using Baculoviral Display

Hideki Kakutani[1☯], Azusa Takahashi[1☯], Masuo Kondoh[1]*, Yumiko Saito[1], Toshiaki Yamaura[1], Toshiko Sakihama[2], Takao Hamakubo[2], Kiyohito Yagi[1]*

1 Laboratory of Bio-Functional Molecular Chemistry, Graduate School of Pharmaceutical Sciences, Osaka University, Suita, Osaka, Japan, **2** Department of Molecular Biology and Medicine, Research Center for Advanced Science and Technology, The University of Tokyo, Meguro, Tokyo, Japan

Abstract

Recent progress in cell biology has provided new insight into the claudin (CL) family of integral membrane proteins, which contains more than 20 members, as a target for pharmaceutical therapy. Few ligands for CL have been identified because it is difficult to prepare CL in an intact form. In the present study, we developed a method to screen for CL binders by using the budded baculovirus (BV) display system. CL4-displaying BV interacted with a CL4 binder, the C-terminal fragment of *Clostridium perfringens* enterotoxin (C-CPE), but it did not interact with C-CPE that was mutated in its CL4-binding region. C-CPE did not interact with BV and CL1-displaying BV. We used CL4-displaying BV to select CL4-binding phage in a mixture of a scFv-phage and C-CPE-phage. The percentage of C-CPE-phage in the phage mixture increased from 16.7% before selection to 92% after selection, indicating that CL-displaying BV may be useful for the selection of CL binders. We prepared a C-CPE phage library by mutating the functional amino acids. We screened the library for CL4 binders by affinity to CL4-displaying BV, and we found that the novel CL4 binders modulated the tight-junction barrier. These findings indicate that the CL-displaying BV system may be a promising method to produce a novel CL binder and modulator.

Citation: Kakutani H, Takahashi A, Kondoh M, Saito Y, Yamaura T, et al. (2011) A Novel Screening System for Claudin Binder Using Baculoviral Display. PLoS ONE 6(2): e16611. doi:10.1371/journal.pone.0016611

Editor: Vladimir Uversky, University of South Florida College of Medicine, United States of America

Received November 22, 2010; **Accepted** December 24, 2010; **Published** February 14, 2011

Funding: This work was supported by a Grant-in-Aid for Scientific Research from the Ministry of Education, Culture, Sports, Science and Technology, Japan (21689006), by a Health and Labor Sciences Research Grant from the Ministry of Health, Labor and Welfare of Japan, by Takeda Science Foundation, by a Suzuken Memorial Foundation, by a grant from Kansai Biomedical Cluster project in Saito, which is promoted by the Knowledge Cluster Initiative of the Ministry of Education, Culture, Sports, Science and Technology, Japan and by a Research Grant for Promoting Technological Seeds from Japan Science and Technology Agency. A.T. is supported by Research Fellowships of the Japan Society for the Promotion of Science for Young Scientists. The funders had no role in study design, data collection and analysis, decision to publish, or preparation of the manuscript.

Competing Interests: The authors have declared that no competing interests exist.

* E-mail: masuo@phs.osaka-u.ac.jp (MK); yagi@phs.osaka-u.ac.jp (KY)

☯ These authors contributed equally to this work.

Introduction

Tight junctions (TJ) are intercellular adhesion complexes in epithelial and endothelial cells; TJs are located in the most apical part of the complexes [1]. TJs have a barrier function and a fence function [2–4]. TJs contribute to epithelial and endothelial barrier functions by restricting the diffusion of solutes through the paracellular pathway. TJs maintain cellular polarity by preventing the free movement of membrane proteins between the apical and basal membranes [5]. Loss of cell-cell adhesion and cellular polarity commonly occurs in the early stages of cancer [6]. Modulation of the TJ barrier function can be a method to enhance drug absorption, and TJ components exposed on the surface of cancer cells can be a target for cancer therapy.

Biochemical analyses of TJs have identified TJ components, such as occludin, claudins (CLs) and junction adhesion molecule [7]. The CL family contains more than 20 integral tetra-transmembrane proteins that play pivotal roles in the TJ barrier and fence functions. CL1-deficient mice lack the epidermal barrier, while CL5-deficient mice lack the blood-brain barrier [8,9], indicating that the regulation of the TJ barrier by modulation of CLs may be a promising method for drug delivery. *Clostridium perfringens* enterotoxin (CPE) causes food poisoning in humans [10]. An interaction between the C-terminal domain of CPE (C-CPE) with CL4 deregulates the TJ barrier [11,12]. We previously found that C-CPE enhances jejunal absorption through its interaction with CL4, indicating that a CL binder is a potent drug-delivery system [13].

The majority of lethal cancers are derived from epithelial tissues [14]. Malignant tumor cells frequently exhibit abnormal TJ function, followed by the deregulation of cellular polarity and intercellular contact, which is commonly observed in both advanced tumors and the early stages of carcinogenesis [6]. Some CLs are overexpressed in various types of cancers. For example, CL3 and CL4 are overexpressed in breast, prostate, ovarian, pancreatic and gastric cancers. CL1, CL7, CL10 and CL16 are overexpressed in colon, gastric, thyroid and ovarian cancers, respectively [15,16]. These findings indicate that the CLs may be a target molecule for cancer therapy. A receptor for CPE is CL4 [11,12]. CPE has anti-tumor activity against human pancreatic and ovarian cancers without side effects [17,18]. The CLs binders will be useful for cancer-targeting therapy.

As above, recent investigations of CLs provide new insight into their use as pharmaceutical agents; for example, a CL binder may be used in drug delivery and anti-tumor therapy. Selection of a CL binder by using a recombinant CL protein is a putative method to

prepare a CL binder. However, CLs are four-transmembrane proteins with high hydrophobicity; there has been little success in the preparation of intact CL protein. Recently, a novel type of protein expression system that uses baculovirus has been developed. Membrane proteins are displayed on the budded baculovirus (BV) in their active form [19–21], indicating that the BV system may be useful for the preparation of a CL binder. In the present study, we investigated whether a CL binder was screened by using a CL-displaying BV.

Results

Preparation of CL4-displaying BV

C-CPE is the only known CL binder and modulator [12,13,22]. C-CPE has affinity to CL4 in a nanomolar range [23]. We chose C-CPE and CL4 as models of the CL binder and CL, respectively. Several reports indicate that membrane proteins expressed on the surface of BV are in an intact form [19–21]. To check the expression of CL4 on the BV, we performed immunoblot analysis of the lysate of CL4-BV against CL4. As shown in Fig. 1A, CL4 was detected in the virus lysates. To determine if the CL4 expressed on the virus has an intact form, we performed enzyme-linked immunosorbent assay (ELISA) with CL4-BV-coated immunoplates. C-CPE binds to the extracellular loop domain of CL4 [23]. After the addition of C-CPE to the CL4-BV-coated plate, the C-CPE bound to the CL4-BV-coated plate was detected by anti-his-tag antibody, followed by incubation with horseradish peroxidase-labeled antibody. C-CPE was dose-dependently bound to CL4-BV, whereas C-CPE did not interact with wild-BV (Fig. 1B). Deletion of the CL4-binding region (C-CPE303) attenuated the interaction of C-CPE with CL4-BV (Fig. 1C). Together, these results indicate that the CL4 displayed on BV may have an intact extracellular loop region.

Selection of C-CPE-phage by using CL4-BV

We next examined the interaction between C-CPE-phage and CL4-BV. As shown in Fig. 2A, C-CPE-phage bound to CL4-BV but not to wild-BV, and a scFv-phage did not bind to CL4-BV. To determine if CL-BV can be used to select CL binders, we prepared a mixture of C-CPE-phage and scFv-phage at a ratio of 2:10 and used CL4-BV to select CL4-binding phage in the mixtures. The amount of C-CPE-phage was increased to 11 of 12 clones in the mixture (Fig. 2B), indicating that CL-BV may be useful in the preparation of CL binders.

We previously found that each substitution of S304, S305, S307, N309, S313 and K318 with alanine increased the binding of C-CPE to CL4 [24]. Here, we prepared a phage library for C-CPE by randomly changing the functional 6 amino acids to any of the 20 amino acids. To confirm the diversity of the library, we checked the sequences of 17 randomly isolated clones. Each of the 17 clones had a different sequence, indicating that the library has a diverse population of C-CPE mutants (Table 1).

Then, we screened the CL4-binding phage by their affinity to CL4-BV. After addition of the C-CPE library to CL4-BV-adsorbed tubes, the CL4-BV-bound phages were recovered (1st screening). We repeated this screening process two more times (2nd screening and 3rd screening). If the number of CL4-bound phage is increased during the screening, the ratio of the incubated phage titers to the recovered phage titers will increase. As shown in Fig. 3A, the ratio was increased during screening from 4.5×10^{-7} to 5.5×10^{-5}, indicating that the screening system for CL4 binders may work. Indeed, the number of monoclonal phage clones with high affinity to CL4-BV was increased after the 3rd screening compared with that after the 2nd screening (Fig. 3B).

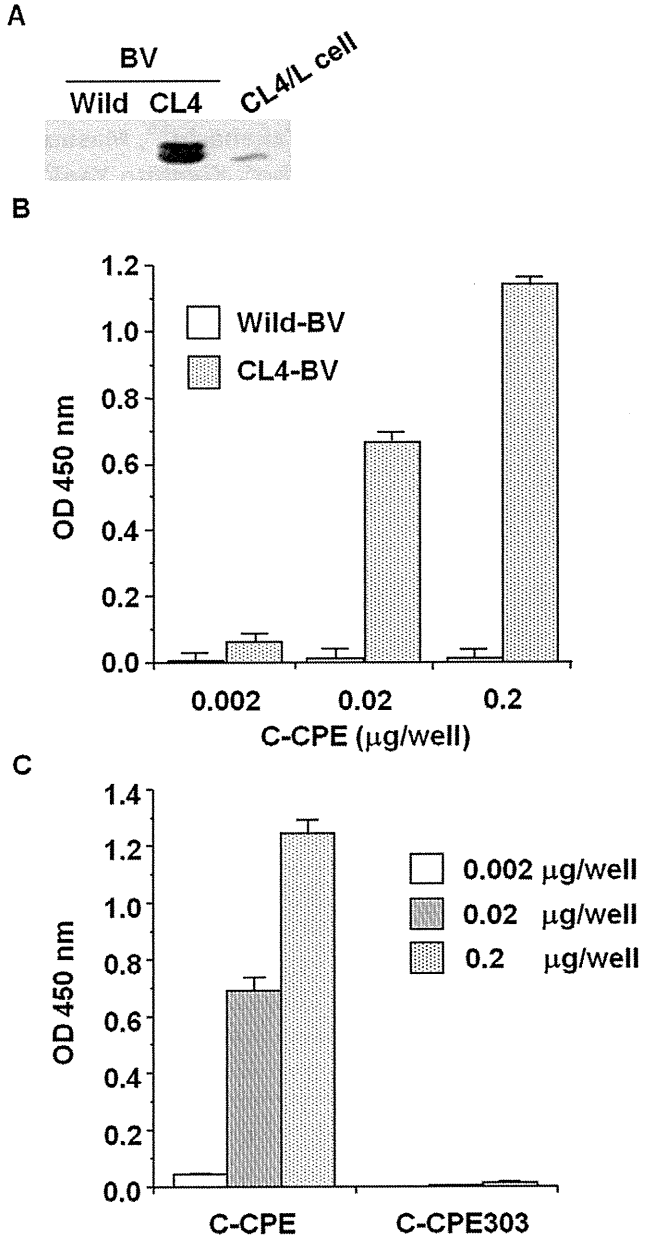

Figure 1. Preparation of CL4-displaying BV. A) Immunoblot analysis. Wild-BV and CL4-BV (0.1 μg/lane) were subjected to SDS-PAGE, followed by immunoblot analysis with anti-CL4 antibody. The lysate of CL4-expressing L (CL4/L) cells was used as a positive control. B, C) Interaction of a CL4 binder with CL4-BV. Immunotubes were coated with the wild-BV or CL4-BV, and C-CPE (B) or mutated C-CPE (C) was added to the BV-coated immunotubes at the indicated concentration. C-CPE bound to the BV-coated tubes was detected by ELISA with an anti-his-tag antibody.
doi:10.1371/journal.pone.0016611.g001

We analyzed the sequences of the CL4-BV-bound phages and got novel CL4-binder candidates with amino acid sequences that differed from the wild-type sequence (Table 2). To investigate their CL4-binding, we prepared the recombinant proteins of the binders and investigated their interaction with CL4 by ELISA with CL-BVs. As shown in Fig. 4A, the novel C-CPE derivatives had affinity to CL4 but not CL1. Next, we investigated whether the novel CL4 binders modulate TJ barrier in Caco-2 monolayer cell sheets, a popular model for the evaluation of TJ barriers [25].

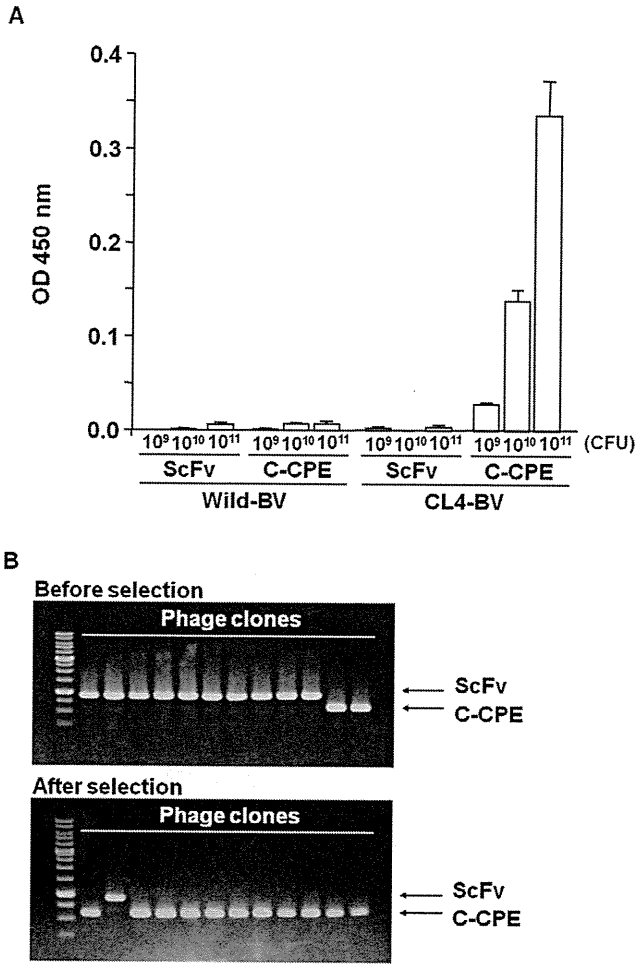

Figure 2. Selection of C-CPE-displaying phage by using the CL4-BV system. A) Interaction of C-CPE-displaying phage with CL4-BV. Wild-BV or CL4-BV was coated on an immunoplate, and then scFv-displaying phage or C-CPE-displaying phage was added to the BV-coated immunoplate at the indicated concentrations. The BV-bound phages were detected by ELISA with anti-M13 antibody as described in Materials and methods. Data are representative of two independent experiments. Data are means ± SD (n = 3). B) Enrichment of C-CPE-displaying phage by the BV system. A mixture of scFv-phage and C-CPE-phage (mixing ratio of scFv-phage to C-CPE-phage = 2:10) was incubated with a CL4-BV-coated immunotube, and the bound phages were recovered. Each phage clone was identified by PCR amplification, followed by agarose gel electrophoresis. Upper and lower pictures are before and after the selection, respectively. The putative sizes of the PCR products are 856 and 523 bp in scFv and C-CPE, respectively. The data are representative of two independent experiments.
doi:10.1371/journal.pone.0016611.g002

Treatment of the cells with C-CPE resulted in decreased transepithelial electrical resistance (TEER) values, a marker of TJ integrity, and the TEER values increased after removal of C-CPE. The C-CPE derivatives (clones 1–5) had TJ-modulating activity similar to that of C-CPE (Fig. 4B).

Discussion

CL is a promising target for pharmaceutical therapy. However, CL has low antigenicity, and there has been little success in the preparation of monoclonal antibody against the extracellular loop region of CL. The three-dimensional structure of CL has never been determined, so it is impossible to perform a theoretical design of a CL binder based on the structural information. In the present study, we developed a novel screening system for CL binders by using a BV system and a C-CPE phage display library, and we used this system to identify novel CL4 binders.

Table 1. C-CPE phage library.

	304	305	307	309	313	318
C-CPE	**S**	**S**	**S**	**N**	**S**	**K**
Clone 1	V	T	C	V	N	K
2	C	P	A	H	L	T
3	A	G	G	V	P	P
4	R	G	H	L	E	H
5	A	A	P	S	R	Q
6	P	A	P	D	P	A
7	C	T	T	T	N	K
8	H	P	S	P	G	H
9	R	G	G	R	N	R
10	A	P	S	T	Q	P
11	V	L	G	N	M	R
12	P	P	A	T	F	R
13	G	D	C	S	N	L
14	F	R	V	F	R	N
15	S	Q	Q	W	T	T
16	S	R	L	E	W	Q
17	K	R	E	R	Q	S

Phage clones were randomly picked up from the C-CPE phage library, and the amino acids sequences of C-CPE mutant were analyzed.
doi:10.1371/journal.pone.0016611.t001

In ligand screening, the preparation of a receptor for the ligand is very critical. Membrane proteins are especially difficult to prepare as recombinant protein with an intact structure. Functional membrane proteins such as cell-surface proteins are heterologously expressed on BV in their native forms [19–21]. Interactions between membrane proteins can be detected by using receptor-displaying and ligand-displaying BV [21]. In the present report, we found that CL4-BV interacts with a CL4 binder, C-CPE, but it does not interact with C-CPE303 that lacks the CL4-binding residues of C-CPE. The CL4-binding site of C-CPE corresponds to that of CPE; so, the second extracellular loop of CL appears to be the C-CPE-binding site [23,26]. These findings indicate that CL4 displayed on BV may have native form. We anticipate that CL-BV will be useful for the preparation of CL binders, such as peptides and antibodies.

To the best of our knowledge, the preparation of CL binder has been performed by only four groups. Offner et al. prepared polyclonal antibodies against extracellular domains of CL3 and CL4 [27], Ling et al. screened peptide types of CL4 binder by using a 12-mer peptide phage display library and CL4-expressing cells [28], Suzuki et al. generated a monoclonal antibody against the second extracellular loop of CL4 from mice immunized with a human pancreatic cancer cell line [29] and Romani et al. screened scFv against CL3 by using a human antibody phage display library [30]. However, the CL modulators have never been developed; thus, C-CPE is the only known CL4 modulator [12]. In the present study, we prepared a C-CPE phage library containing C-CPE mutants in which each of the 6 functional amino acids was randomly replaced with an amino acid, and we isolated CL4 binders by using CL4-BV as a screening ligand. Interestingly, all of

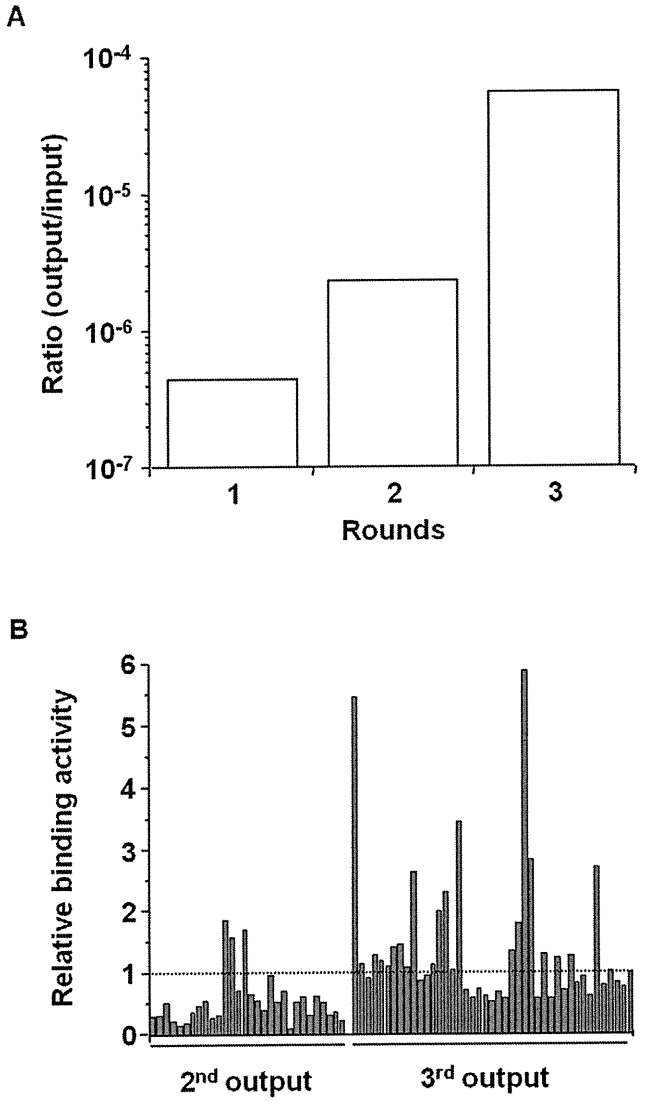

Figure 3. Screening of a novel CL4 binder. A) Enrichment of phages with affinity to CL4-BV. CL4-BVs coated on immunotubes were incubated with the C-CPE-derivative phage library at 1.6×10^{12} CFU titer (1^{st} input phage). The phages bound to CL4-BV were recovered (1^{st} output phage). The CL4-BV-binding phages were subjected to two additional cycles of the incubation and wash step, resulting in 2^{nd}, 3^{rd} output phage. The ratio of output phage to input phage titers was calculated. B) Monoclonal analysis of C-CPE-derivative phage. CL4-BV-bound phage clones were isolated from the 2^{nd} and 3^{rd} output phages, and the interaction of the monoclonal phage with CL4-BV was examined by ELISA with anti-M13 antibody as described in Materials and methods. Data are expressed as relative binding to that of C-CPE-phage indicated by the most right column.
doi:10.1371/journal.pone.0016611.g003

the CL4 binders modulated TJ barriers. We are investigating why the substitution of the amino acids with the other amino acids modulated CL4. These findings indicate that a BV screening system with a C-CPE library may be a powerful method to develop CL modulators.

The CL family forms various types of TJ barriers through combinations of its more than 20 members in homophilic/heterophilic CL strands [31,32]. Intercellular proteins ZO-1 and ZO-2 determine the localization of CL strands [33]. If a screening system to reconstitute heterogeneous CL strands with ZO-1 and/or ZO-2 is developed, then useful and effective CL modulators can be identified. In this point, the BV system has extremely superior features. G protein and G protein-coupled receptors have been

Table 2. CL4-binding phages.

	304	305	307	309	313	318
C-CPE	S	S	S	N	S	K
Clone 1	R	V	S	A	R	R
2	R	S	V	A	R	K
3	G	D	G	R	T	R
4	S	A	P	R	S	A
5	R	S	L	K	S	K

The sequences of C-CPE mutant in the CL4-binding phages were analyzed.
doi:10.1371/journal.pone.0016611.t002

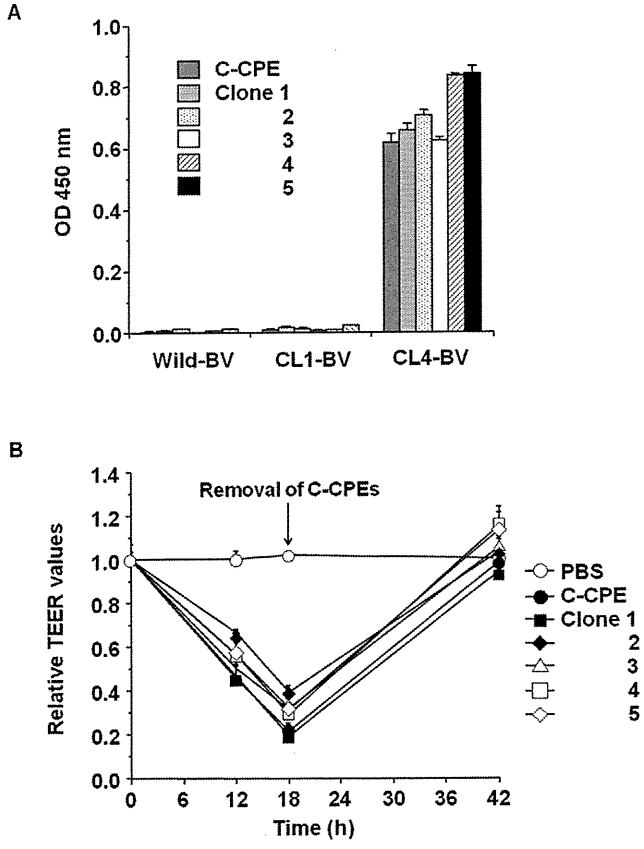

Figure 4. Isolation of a novel CL4 modulator. A) Interaction of the C-CPE derivatives with CL4. C-CPE derivatives were prepared as his-tagged recombinant proteins. The C-CPE derivatives (0.02 μg) were added to CL-BV-coated immunoplates, followed by detection of the C-CPE derivatives bound to CL-BV. Data are means ± SD (n = 4). B) Modulation of tight junction-barriers. Caco-2 cells were cultured on Transwell™ chambers. When TEER values reach a plateau, the cells were treated with C-CPE or C-CPE derivatives at the indicated concentrations. After 18 h of exposure to the C-CPEs, the cells were washed with medium to remove C-CPEs, and then the cells were cultured for an additional 24 h. Changes in TEER values were monitored during the C-CPEs treatment. Relative TEER values were calculated as the ratio of TEER values at 0 h. Data are representative of two independent experiments. The data are means ± SD (n = 4).
doi:10.1371/journal.pone.0016611.g004

functionally reconstituted in BV [20,34], and functional γ-secretase complexes have also been reconstituted on BV [35]. In the near future, the reconstituted CL system on BV will be developed and used for the screening of CL binders and modulators, hopefully leading to breakthroughs in pharmaceutical therapies that target CLs.

Materials and Methods

Recombinant BV construction and Sf9 cell culture

Recombinant BV was prepared by using the Bac-to-Bac expression system, according to the manufacturer's instructions (Invitrogen, Gaithersburg, MD). Briefly, mouse CL1 and CL4 cDNA (kind gifts from Dr. M Furuse, Kobe University, Japan) were inserted into pFastBac1, and the resulting plasmids were transduced into DH10Bac *E. Coli* cells. Recombinant bacmid DNA was extracted from the cells. Sf9 cells were transduced with the bacmid coding CL, and the recombinant BV was recovered by centrifugation of the conditioned medium [36].

Preparation of the BV fractions

Sf9 cells (2×10^6 cells) were infected with recombinant BV at a multiplicity of infection of 5. Seventy-two hours after infection, the BV fraction was recovered from the culture supernatant of infected Sf9 cells by centrifugation. The pellets of the BV fraction were resuspended in Tris-buffered saline (TBS) containing 1% protease inhibitor cocktail (Sigma-Aldrich, St. Louis, MO) and then stored at 4°C until use. The expression of CL1 and CL4 in the BV was confirmed by sodium dodecyl sulfate-polyacrylamide gel electrophoresis (SDS-PAGE) and immunoblot analysis with anti-CL antibodies (Zymed Laboratory, South San Francisco, CA).

Preparation of mutant C-CPE library

C-CPE fragments in which the functional amino acids (S304, S305, S307, N309, S313 and K318) [24] were randomly mutated were prepared by polymerase chain reaction (PCR) with pET-H_{10}PER as a template, a forward primer (5′-catgccatggccgatatagaaaaagaaatccttgatttagctgctg-3′, Nco I site is underlined) and a reverse primer (5′-ttttccttttgcggccgcaaa*nn*ttgaaataatat*nn*ataagggta*nn*tcc*nn*ata*nnnnn*attagcttt-3′, Not I site is underlined, and the randomly mutated amino acids are in italics). The PCR fragments were inserted into a pY03 phagemid at the NcoI/NotI sites [22]. The resultant phagemid containing the C-CPE mutant library was transduced into *E. coli* TG1 cells, and then the cells were stored at −80°C.

Preparation of phage

TG1 cells containing phagemid coding a scFv, C-CPE, C-CPE mutant or C-CPE mutant library were culture in 2YT medium containing 2% glucose and ampicillin. When the cells grew to a growing phage, M13K07 helper phages (Invitrogen) were added, and the medium was changed into 2YT medium containing ampicillin and kanamycin. After an additional 6 h of culture, the phages in the conditioned medium were precipitated with polyethylene glycol. The phages were suspended in phosphate-buffered saline (PBS) and stored at 4°C until use.

ELISA

Wild-BVs or CL-BVs (0.5 μg/well) were adsorbed onto an immunoplate (Greiner Bio-One, Frickenhausen, Germany). The wells were washed with PBS and blocked with TBS containing 1.6% BlockAce (Dainippon Sumitomo Pharma, Osaka, Japan). C-CPEs or phages were incubated in the immunoplate, and the BV-bound C-CPEs or phages were detected by using anti-his-tag antibody (Novagen, Darmstadt, Germany) or anti-M13 antibody (Amersham-Pharmacia Biotech, Uppsala, Sweden), respectively, horseradish peroxidase-labelled secondary antibody and TMB peroxidase substrate (Nacalai Tesque, Kyoto, Japan). The immunoreactive C-CPEs or phages were quantified by the measurement of absorbance at 450 nm. In the screening of phages, the data were normalized by the amounts of phages, which were quantified by ELISA for the FLAG-tag contained in the coat protein.

Selection of phage by using BV

A total of 0.5 μg of BV was adsorbed onto an immunotube (Nunc, Roskilde, Denmark). The tube was washed with PBS and blocked with TBS containing 4.0% BlockAce. The BV-coated tubes were incubated with mixture of phages, and then the tubes were washed 15 times with PBS and 15 times with PBS containing 0.05% Tween 20. The phages bound to the tube were eluted with 100 mM HCl. TG1 cells were infected with the eluted phages, and phages were prepared as described above. The resulting phages were subjected to repeated selection by using the BV-coated immunotubes.

Identification of a phage clone

To identify an isolated phage clone, we performed PCR or sequencing analysis. We amplified the inserted fragment into the phagemid by PCR using forward primer 5′-caggaaacagctatgac-3′ and reverse primer 5′-gtaaatgaattttctgtatgagg-3′. The resultant PCR products were subjected to agarose gel electrophoresis followed by staining with ethidium bromide. We performed a sequence analysis with primer 5′-gtaaatgaattttctgtatgagg-3′.

Measurement of phage titer

To quantify the concentration of phages, we measured the titer (colony formation unit (CFU)/ml) of the phage solution. Briefly, the phage solution was diluted to 10^{-5}–10^{-10} with PBS. The diluted solution was seeded onto Petrifilm™ (Tech-Jam, Osaka, Japan). After 24 h of incubation, the colonies were counted, and the titer was calculated.

Purification of C-CPE mutants

C-CPE and C-CPE303, in which the CL-4 binding region of C-CPE was deleted, were prepared as described previously [13]. To prepare plasmid containing C-CPE mutants, the C-CPE mutant fragment was PCR-amplified by using phagemids coding C-CPE mutants as a template. The resulting PCR fragment was inserted into pET16b, and the sequence was confirmed. The plasmids were transduced into *E. coli* strain BL21 (DE3), and production of mutant C-CPEs was induced by the addition of isopropyl-D-thiogalactopyranoside. The harvested cells were lysed in buffer A (10 mM Tris-HCl, pH 8.0, 400 mM NaCl, 5 mM $MgCl_2$, 0.1 mM phenylmethanesulfonyl fluoride, 1 mM 2-mercaptoethanol, and 10% glycerol) that was supplemented with 8 M urea when necessary. The lysates were applied to HiTrap™ Chelating HP (GE Healthcare, Buckinghamshire, UK), and mutant C-CPEs were eluted with buffer A containing 100–400 mM imidazole. The buffer was exchanged with PBS by using a PD-10 column (GE Healthcare), and the purified protein was stored at −80°C until use. Purification of the mutant C-CPEs was confirmed by SDS-PAGE, followed by staining with Coomassie Brilliant Blue and by immunoblotting with anti-his-tag antibody (Novagen). Protein was quantified by using a BCA protein assay kit with bovine serum albumin as a standard (Pierce Chemical, Rockford, IL).

TEER assay

Caco-2 cells were seeded in Transwell^{TM} chambers (Corning, NY) at a subconfluent density. The TEER of the Caco-2 monolayer cell sheets on the chamber was monitored by using a Millicell-ERS epithelial volt-ohmmeter (Millipore, Billerica, MA). When TEER values reached a plateau, indicating that TJs were well-developed in the cell sheets, the Caco-2 monolayers were treated with C-CPE or C-CPE mutants on the basal side of the chamber. Changes in TEER values were monitored. The TEER values were normalized by the area of the Caco-2 monolayer, and the TEER value of a blank Transwell^{TM} chamber (background) was subtracted.

Acknowledgments

We thank Drs. S. Tsunoda (National Institute of Biomedical Innovation, Japan), Y. Tsutsumi, Y. Mukai (Osaka University, Japan) for their kind instruction of phage display technology. We also thank Drs. Y. Horiguchi (Osaka University, Japan), S. Tsukita (Kyoto University, Japan) and members of our laboratory for providing us C-CPE cDNA, CL-expressing cells and their useful comments and discussion, respectively.

Author Contributions

Conceived and designed the experiments: MK TS TH KY. Performed the experiments: HK AT MK YS TY TS. Analyzed the data: HK AT MK KY. Contributed reagents/materials/analysis tools: HK AK TS TH. Wrote the manuscript: HK MK TY.

References

1. Farquhar MG, Palade GE (1963) Junctional complexes in various epithelia. J Cell Biol 17: 375–412.
2. Anderson JM, Van Itallie CM, Fanning AS (2004) Setting up a selective barrier at the apical junction complex. Curr Opin Cell Biol 16: 140–145.
3. Balda MS, Matter K (1998) Tight junctions. J Cell Sci 111(Pt 5): 541–547.
4. Tsukita S, Furuse M, Itoh M (2001) Multifunctional strands in tight junctions. Nat Rev Mol Cell Biol 2: 285–293.
5. Mitic LL, Anderson JM (1998) Molecular architecture of tight junctions. Annu Rev Physiol 60: 121–142.
6. Wodarz A, Nathke I (2007) Cell polarity in development and cancer. Nat Cell Biol 9: 1016–1024.
7. Schneeberger EE, Lynch RD (2004) The tight junction: a multifunctional complex. Am J Physiol 286: C1213–C1228.
8. Furuse M, Hata M, Furuse K, Yoshida Y, Haratake A, et al. (2002) Claudin-based tight junctions are crucial for the mammalian epidermal barrier: a lesson from claudin-1-deficient mice. J Cell Biol 156: 1099–1111.
9. Nitta T, Hata M, Gotoh S, Seo Y, Sasaki H, et al. (2003) Size-selective loosening of the blood-brain barrier in claudin-5-deficient mice. J Cell Biol 161: 653–660.
10. McClane BA (1994) *Clostridium perfringens* enterotoxin acts by producing small molecule permeability alterations in plasma membranes. Toxicology 87: 43–67.
11. Katahira J, Inoue N, Horiguchi Y, Matsuda M, Sugimoto N (1997) Molecular cloning and functional characterization of the receptor for *Clostridium perfringens* enterotoxin. J Cell Biol 136: 1239–1247.
12. Sonoda N, Furuse M, Sasaki H, Yonemura S, Katahira J, et al. (1999) *Clostridium perfringens* enterotoxin fragment removes specific claudins from tight junction strands: Evidence for direct involvement of claudins in tight junction barrier. J Cell Biol 147: 195–204.
13. Kondoh M, Masuyama A, Takahashi A, Asano N, Mizuguchi H, et al. (2005) A novel strategy for the enhancement of drug absorption using a claudin modulator. Mol Pharmacol 67: 749–756.
14. Jemal A, Siegel R, Ward E, Hao Y, Xu J, et al. (2008) Cancer statistics, 2008. CA Cancer J Clin 58: 71–96.
15. Kominsky SL (2006) Claudins: emerging targets for cancer therapy. Expert Rev Mol Med 8: 1–11.
16. Morin PJ (2005) Claudin proteins in human cancer: promising new targets for diagnosis and therapy. Cancer Res 65: 9603–9606.
17. Michl P, Buchholz M, Rolke M, Kunsch S, Lohr M, et al. (2001) Claudin-4: a new target for pancreatic cancer treatment using *Clostridium perfringens* enterotoxin. Gastroenterology 121: 678–684.
18. Santin AD, Cane S, Bellone S, Palmieri M, Siegel ER, et al. (2005) Treatment of chemotherapy-resistant human ovarian cancer xenografts in C.B-17/SCID mice by intraperitoneal administration of *Clostridium perfringens* enterotoxin. Cancer Res 65: 4334–4342.
19. Loisel TP, Ansanay H, St-Onge S, Gay B, Boulanger P, et al. (1997) Recovery of homogeneous and functional beta 2-adrenergic receptors from extracellular baculovirus particles. Nat Biotechnol 15: 1300–1304.
20. Sakihama T, Masuda K, Sato T, Doi T, Kodama T, et al. (2008) Functional reconstitution of G-protein-coupled receptor-mediated adenylyl cyclase activation by a baculoviral co-display system. J Biotechnol 135: 28–33.
21. Sakihama T, Sato T, Iwanari H, Kitamura T, Sakaguchi S, et al. (2008) A simple detection method for low-affinity membrane protein interactions by baculoviral display. PLoS ONE 3: e4024.
22. Ebihara C, Kondoh M, Hasuike N, Harada M, Mizuguchi H, et al. (2006) Preparation of a claudin-targeting molecule using a C-terminal fragment of *Clostridium perfringens* enterotoxin. J Pharmacol Exp Ther 316: 255–260.
23. Fujita K, Katahira J, Horiguchi Y, Sonoda N, Furuse M, et al. (2000) *Clostridium perfringens* enterotoxin binds to the second extracellular loop of claudin-3, a tight junction integral membrane protein. FEBS Lett 476: 258–261.
24. Takahashi A, Komiya E, Kakutani H, Yoshida T, Fujii M, et al. (2008) Domain mapping of a claudin-4 modulator, the C-terminal region of C-terminal fragment of *Clostridium perfringens* enterotoxin, by site-directed mutagenesis. Biochem Pharmacol 75: 1639–1648.
25. Meunier V, Bourrie M, Berger Y, Fabre G (1995) The human intestinal epithelial cell line Caco-2; pharmacological and pharmacokinetic applications. Cell Biol Toxicol 11: 187–194.
26. Hanna PC, Mietzner TA, Schoolnik GK, McClane BA (1991) Localization of the receptor-binding region of *Clostridium perfringens* enterotoxin utilizing cloned toxin fragments and synthetic peptides. J Biol Chem 266: 11037–11043.
27. Offner S, Hekele A, Teichmann U, Weinberger S, Gross S, et al. (2005) Epithelial tight junction proteins as potential antibody targets for pancarcinoma therapy. Cancer Immunol Immunother 54: 431–445.
28. Ling J, Liao H, Clark R, Wong MS, Lo DD (2008) Structural constraints for the binding of short peptides to claudin-4 revealed by surface plasmon resonance. J Biol Chem 283: 30585–30595.
29. Suzuki M, Kato-Nakano M, Kawamoto S, Furuya A, Abe Y, et al. (2009) Therapeutic antitumor efficacy of monoclonal antibody against Claudin-4 for pancreatic and ovarian cancers. Cancer Sci 100: 1623–1630.
30. Romani C, Comper F, Bandiera E, Ravaggi A, Bignotti E, et al. (2009) Development and characterization of a human single-chain antibody fragment against claudin-3: a novel therapeutic target in ovarian and uterine carcinomas. Am J Obstet Gynecol 201: 70 e71–79.
31. Furuse M, Furuse K, Sasaki H, Tsukita S (2001) Conversion of zonulae occludentes from tight to leaky strand type by introducing claudin-2 into Madin-Darby canine kidney I cells. J Cell Biol 153: 263–272.
32. Furuse M, Sasaki H, Tsukita S (1999) Manner of interaction of heterogeneous claudin species within and between tight junction strands. J Cell Biol 147: 891–903.
33. Umeda K, Ikenouchi J, Katahira-Tayama S, Furuse K, Sasaki H, et al. (2006) ZO-1 and ZO-2 independently determine where claudins are polymerized in tight-junction strand formation. Cell 126: 741–754.
34. Masuda K, Itoh H, Sakihama T, Akiyama C, Takahashi K, et al. (2003) A combinatorial G protein-coupled receptor reconstitution system on budded baculovirus. J Biol Chem 278: 24552–24562.
35. Hayashi I, Urano Y, Fukuda R, Isoo N, Kodama T, et al. (2004) Selective reconstitution and recovery of functional gamma-secretase complex on budded baculovirus particles. J Biol Chem 279: 38040–38046.
36. Saeki R, Kondoh M, Kakutani H, Tsunoda S, Mochizuki Y, et al. (2009) A novel tumor-targeted therapy using a claudin-4-targeting molecule. Mol Pharmacol 76: 918–926.

Hindawi Publishing Corporation
Journal of Drug Delivery
Volume 2011, Article ID 203986, 7 pages
doi:10.1155/2011/203986

Research Article

Local Gene Delivery System by Bubble Liposomes and Ultrasound Exposure into Joint Synovium

Yoichi Negishi,[1] Yuka Tsunoda,[1] Yoko Endo-Takahashi,[1] Yusuke Oda,[2] Ryo Suzuki,[2] Kazuo Maruyama,[2] Matsuo Yamamoto,[3] and Yukihiko Aramaki[1]

[1] *Department of Drug and Gene Delivery Systems, School of Pharmacy, Tokyo University of Pharmacy and Life Sciences, 1432-1 Horinouchi, Hachioji, Tokyo 192-0392, Japan*
[2] *Department of Biopharmaceutics, Teikyo University, 1091-1 Suwarashi, Midori-ku, Sagamihara, Kanagawa 252-5195, Japan*
[3] *Department of Periodontology, Showa University School of Dentistry, 2-1-1 Kitasenzoku, Ohta-ku, Tokyo 145-8515, Japan*

Correspondence should be addressed to Yoichi Negishi, negishi@toyaku.ac.jp

Received 17 January 2011; Accepted 1 March 2011

Academic Editor: Susan Hua

Recently, we have developed novel polyethylene glycol modified liposomes (bubble liposomes; BL) entrapping an ultrasound (US) imaging gas, which can work as a gene delivery tool with US exposure. In this study, we investigated the usefulness of US-mediated gene transfer systems with BL into synoviocytes *in vitro* and joint synovium *in vivo*. Highly efficient gene transfer could be achieved in the cultured primary synoviocytes transfected with the combination of BL and US exposure, compared to treatment with plasmid DNA (pDNA) alone, pDNA plus BL, or pDNA plus US. When BL was injected into the knee joints of mice, and US exposure was applied transcutaneously to the injection site, highly efficient gene expression could be observed in the knee joint transfected with the combination of BL and US exposure, compared to treatment with pDNA alone, pDNA plus BL, or pDNA plus US. The localized and prolonged gene expression was also shown by an *in vivo* luciferase imaging system. Thus, this local gene delivery system into joint synovium using the combination of BL and US exposure may be an effective means for gene therapy in joint disorders.

1. Introduction

Intra-articular gene therapy is considered a feasible technique to deliver therapeutic proteins to suppress inflammation and destruction of the joints in rheumatoid arthritis and osteoarthritis, because it could minimize extra-articular adverse effects linked to the systemic injection of drugs [1, 2]. To achieve successful gene therapy in a clinical setting, it is critical that the gene delivery system is safe, easy to apply, and provides therapeutic transgene expression. Previous studies using viral vectors reported the successful transfer of therapeutic genes into the target cells in joint diseases [1, 2], but because of the considerable immunogenicity related to the use of viruses, nonviral gene transfer still needs to be developed [3]. Recently, it has been reported that therapeutic ultrasound as a physical non-viral gene transfer method enables genes to permeate cell membranes. Acoustic cavitation is involved in the mechanism of gene transfer [4–8]; however, to achieve efficient gene transfer, high intensity ultrasound (US) is needed, leading to tissue damage [9–11]. In contrast, low-intensity US in combination with microbubbles has recently acquired much attention as a safe method of gene delivery [12–16]; however, microbubbles have problems with size, stability, and targeting function. Liposomes have been known as drug, antigen, and gene delivery carriers [17–21]. To solve the above-mentioned issues of microbubbles, we previously developed polyethylene glycol- (PEG-) modified liposomes entrapping echo contrast, bubble liposomes (BL), which can function as a novel gene delivery tool by applying them with US exposure [22–27].

The establishment of a method to deliver genes into joints by the combination of BL and US exposure may facilitate the development of a safe and efficient gene therapy for joint disorders. In the present study, we investigated the usefulness of US-mediated gene transfer systems with BL into synoviocytes *in vitro* and the joint synovium *in vivo*.

2. Materials and Methods

2.1. Preparation of Bubble Liposomes. Bubble liposomes were prepared by the previously described methods [22, 23, 26]. Briefly, PEG liposomes composed of 1,2-dipalmitoyl-*sn*-glycero-3-phosphocholine (DPPC) (NOF Corporation, Tokyo, Japan) and 1,2-distearoyl-*sn*-glycero-3-phosphatidyl-ethanolamine-polyethylen eglycol (DSPE-PEG_{2000}-OMe) (NOF Corporation) in a molar ratio of 94 : 6 were prepared by a reverse phase evaporation method. In brief, the reagents were dissolved 1 : 1 (v/v) in chloroform/diisopropyl ether. Phosphate-buffered saline was added to the lipid solution, and the mixture was sonicated and then evaporated at 47°C. The organic solvent was completely removed, and the size of the liposomes was adjusted to less than 200 nm using extruding equipment and a sizing filter (pore size: 200 nm) (Nuclepore Track-Etch Membrane, Whatman plc, UK). The lipid concentration was measured using a Phospholipid C test Wako (Wako Pure Chemical Industries, Ltd., Osaka, Japan). BL were prepared from liposomes and perfluoropropane gas (Takachio Chemical Ind. Co. Ltd., Tokyo, Japan). First, 2 mL sterilized vials containing 0.8 mL liposome suspension (lipid concentration: 1 mg/mL) were filled with perfluoropropane gas, capped, and then pressurized with a further 3 mL perfluoropropane gas. The vial was placed in a bath-type sonicator (42 kHz, 100 W) (BRANSONIC 2510j-DTH; Branson Ultrasonics Co., Danbury, Conn, USA) for 5 min to form BL.

2.2. Plasmid DNA. The plasmid pCMV-Luc is an expression vector encoding the firefly luciferase gene under the control of a cytomegalovirus promoter. The plasmid pDsRed-Express-N1 (Clontech Laboratories, Inc., Mountain View, Calif, USA) is an expression vector encoding the red fluorescent protein under the control of a cytomegalovirus promoter.

2.3. Transfection of Plasmid DNA into Primary Synoviocytes Using Bubble Liposomes. Primary synoviocytes (HFLS), which are primary fibroblast-like cells derived from the inflamed synovial tissue of rheumatoid arthritis patients, were purchased from Cell Applications, Inc. (San Diego, Calif, USA). The culture was performed according to the manufacturer's instructions. The day before transfection, cells (3×10^4) were seeded in the wells of a 48-well plate (ASAHI TECHNOGLASS CO., Chiba, Japan). Five micrograms of pDNA and 60 μg BL were mixed together with culture medium containing 10% FBS and added to the cells. The cells were immediately exposed to US (frequency, 2 MHz, duty, 50%; burst rate, 2.0 Hz; intensity, 2.5 W/cm^2) for 10 sec through a 6-mm diameter probe placed in the well. A Sonopore 3000 (NEPA GENE, Co., Ltd., Chiba, Japan) was used to generate the US. The cells were washed twice with culture medium and cultured for two days. The cell lysate was prepared with lysis buffer (0.1 M Tris-HCl (pH 7.8), 0.1% Triton X-100, and 2 mM EDTA). Luciferase activity was measured using a luciferase assay system (Promega, Madison, WI) and a luminometer (LB96V; Belthold Japan Co. Ltd., Tokyo, Japan). The activity is indicated as relative light units (RLU) per mg of protein.

2.4. Transfection of Plasmid DNA with Lipofectamine 2000. The day before transfection, HFLS-RA (4×10^4) were seeded in the wells of a 48-well plate (ASAHI TECHNOGLASS CO., Chiba, Japan). Then, 0.25 μg pDNA (final concentration, 25 nM) wsa diluted in Opti-MEM (GIBCO). Next, 1.25 μg Lipofectamine 2000 (LF2000) (Invitrogen Japan K.K., Tokyo, Japan) was diluted in Opti-MEM. These solutions were mixed and added to the cells. After 4 and 24 hours, the cells were washed with PBS and cultured for two days. The experiments were performed according to the manufacturers' instructions.

2.5. Measurement of Luciferase and DsRed Expression. Cell lysate was prepared with lysis buffer (0.1 M Tris-HCl (pH 7.8), 0.1% Triton X-100, and 2 mM EDTA). Luciferase activity was measured using a luciferase assay system (Promega, Madison, WI) and a luminometer (LB96V; Belthold Japan Co. Ltd.). The activity is indicated as relative light units (RLU) per mg protein. To analyze DsRed expression, the treated cells were observed with a fluorescence microscope (Axiovert 200 M; Carl Zeiss).

2.6. In Vivo Gene Delivery into the Joint Synovium of Mice with Bubble Liposomes and Ultrasound Exposure. To determine the efficiency of gene delivery, animals were divided into five experimental groups and one control group ($n = 4$ in each group). ICR mice (5 weeks old, male) were anesthetized with an *i.p.* injection of sodium pentobarbital (80 mg/kg) throughout each procedure. A 40 μL suspension of pDNA (20 μg) and BL (30 μg) was injected into the knee joint of the ICR mice, and US exposure (frequency, 1 MHz; duty, 50%; intensity, 2 W/cm^2; time, 60 sec) was immediately applied at the injection site. Five days after the injection, the mice were euthanized and sacrificed, and the knee joint tissue in the US-exposed area was collected and homogenized. The tissue homogenates were prepared with lysis buffer (0.1 M Tris-HCl (pH 7.8), 0.1% Triton X-100, and 2 mM EDTA). Luciferase activity was measured using a luciferase assay system (Promega, Madison, WI) and a luminometer (LB96V; Belthold Japan Co. Ltd.). Activity is indicated as relative light units (RLU) per mg of protein.

2.7. In Vivo Luciferase Imaging. To determine the efficiency of gene delivery, animals were divided into five experimental groups and one control group ($n = 4$ in each group). ICR mice (5 weeks old, male) were anesthetized with an *i.p.* injection of sodium pentobarbital (80 mg/kg) throughout each procedure. A 40 μL suspension of pDNA (20 μg) and BL (30 μg) was injected into the knee joint of the ICR mice, and US exposure (frequency, 1 MHz; duty, 50%; intensity, 2 W/cm^2; time, 60 sec) was immediately applied at the injection site. Several days after the injection, the mice were anaesthetized and *i.p.* injected with D-luciferin (150 mg/kg) (Xenogen Corporation, Calif, USA). After 10 min, luciferase expression was observed with an *in vivo* luciferase imaging

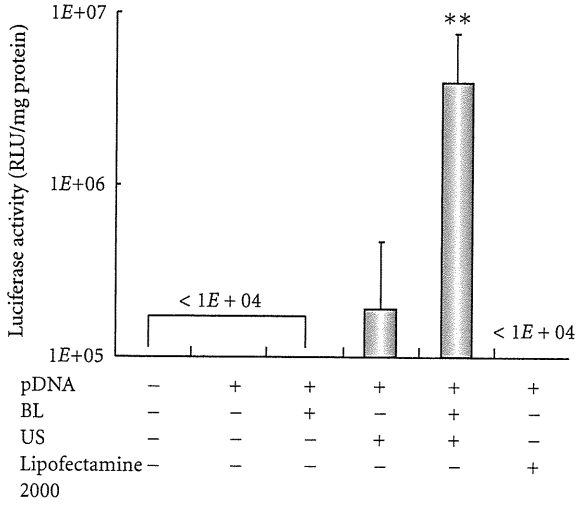

FIGURE 1: Luciferase expression in HFLS transfected with bubble liposomes and ultrasound exposure compared with Lipofectamine 2000. pDNA (pCMV-Luc) and BL were mixed together with culture medium and added to the HFLS. The cells were immediately exposed to US (frequency, 2 MHz; duty, 50%; intensity, 2.5 W/cm^2; US exposure time, 10 sec.). The cells were washed and cultured for 2 days, and then luciferase activity was determined as described in Section 2 . The transfection of pDNA by LF2000 was also performed according to the manufacturers' instructions. All data are shown as the mean ± SD ($n = 4$). $^{**}P < .05$ versus other treatment groups. BL: bubble liposomes; US: ultrasound exposure.

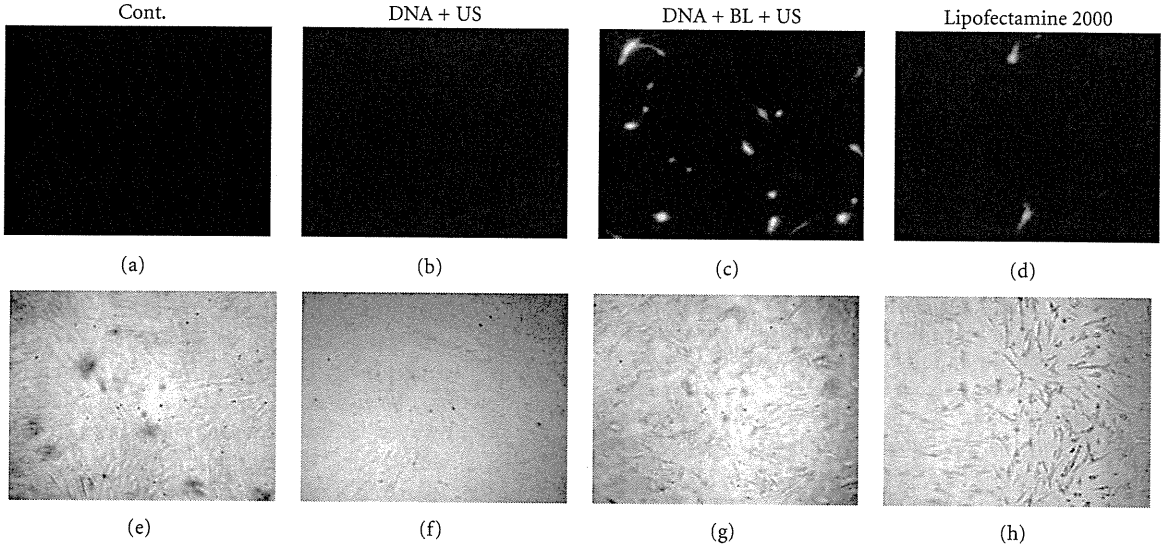

FIGURE 2: DsRed expression in HFLS transfected with bubble liposomes and ultrasound exposure compared with Lipofectamine 2000. pDNA (pDsRed-Express-N1) and BL were mixed together with culture medium and added to the HFLS. The cells were immediately exposed to US (frequency, 2 MHz; duty, 50%; intensity, 2.5 W/cm^2; US exposure time, 10 sec.). The cells were washed and cultured for 2 days and then treated cells were examined by a fluorescence microscope original magnification X200. Transfection of pDNA by LF2000 was also performed. BL: bubble liposomes; US: ultrasound exposure. Fluorescence, (a–d); phase contrast, (e–h).

system (IVIS) (Xenogen Corporation). The image of a representative of the 4 mice was used for each treatment group in this experiment.

2.8. Immunohistochemistry. The gene-transfected joint tissues were preserved in 10% PFA, decalcified with EDTA, and then embedded in paraffin and sectioned. Sections (3 μm thickness) were evaluated for the expression of luciferase protein by immunostaining. The sections were deparaffinized in xylene, rehydrated through graded ethanol, and equilibrated in PBS. The sections were incubated with biotin-labeled rabbit antiluciferase antibody (Cortex Biochem, San Leandro, Calif, USA). The following day, after three washes in PBS, immunoreactivity was detected using an antigoat IgG/HRP and diaminobenzidine (DAB). After color development, the joint sections were counterstained with hematoxylin and were then dehydrated, cleared, and mounted on slides.

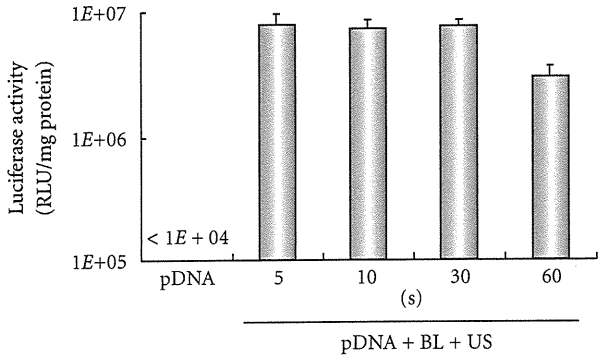

FIGURE 3: Effect of ultrasound exposure time on transfection with bubble liposomes into HFLS. pDNA (pCMV-Luc) and BL were mixed together with culture medium and added to the HFLS. The cells were immediately exposed to US (intensity, 2.5 W/cm^2; US exposure time, 5–60 sec.). The cells were washed and cultured for 2 days, and then luciferase activity was determined. All data are shown as the mean ± SD (n = 4). BL: bubble liposomes; US: ultrasound exposure.

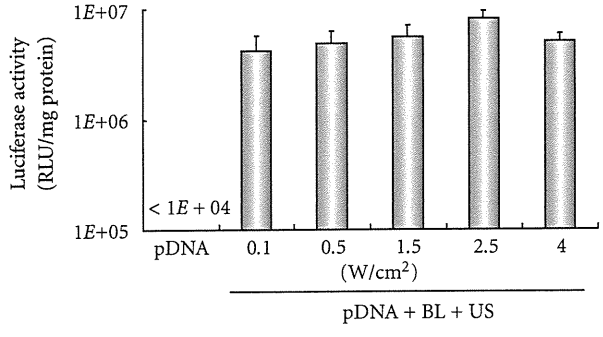

FIGURE 4: Effect of ultrasound intensity on transfection with Bubble liposomes into HFLS. pDNA (pCMV-Luc) and BL were mixed together with culture medium and added to the HFLS. The cells were immediately exposed to US (intensity, 0.1–4 W/cm^2; US exposure time, 10 sec.). The cells were washed and cultured for 2 days and then luciferase activity was determined. All data are shown as the mean ± SD (n = 4). BL: bubble liposomes; US: ultrasound exposure.

2.9. In Vivo Studies. Animal use and relevant experimental procedures were approved by Tokyo University of Pharmacy and Life Science Committee and Teikyo University on the Care and Use of Laboratory Animals. All experimental protocols for animal studies were in accordance with the Principle of Laboratory Animal Care at Teikyo University.

2.10. Statistical Analyses. All data are shown as the mean±SD (n = 4 or 6). Data were considered significant when $P < .05$. The t-test was used to calculate statistical significance.

3. Results and Discussion

3.1. Gene Transfection with Bubble Liposomes and Ultrasound Exposure into Synoviocytes In Vitro. It is known that microbubbles improve cell and tissue permeability by cavitation upon US exposure [11–15]. We first tried

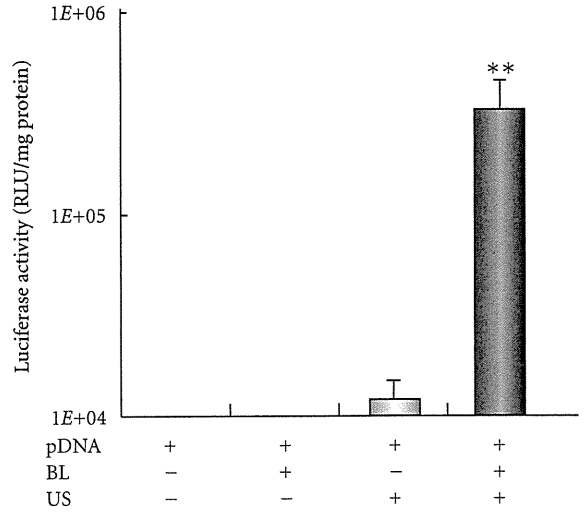

FIGURE 5: *In vivo* luciferase expression in the joint synovium after transfection with bubble liposome and ultrasound exposure. A suspension of pDNA and BL was injected into the knee joint of the mice, and US exposure (frequency, 1 MHz; duty, 50%; intensity, 2 W/cm^2; time, 60 sec) was immediately applied at the injection site. Five days after injection, the knee joint tissue in the US-exposed area was collected and homogenized. Luciferase activity was determined. All data are shown as the mean ± SD (n = 4). $^{**}P < .05$ versus other treatment groups. BL: bubble liposomes; US: ultrasound exposure.

to transfect naked pDNA (pCMV-Luc) into primary synoviocytes (HFLS), which are primary fibroblast-like cells derived from the inflamed synovial tissue of rheumatoid arthritis patients, by BL and/or US (Figure 1). As a result, luciferase activity in the group receiving a combination of BL with US exposure was 400- or 30-fold higher than that of the group treated with pDNA alone or pDNA plus US, respectively (Figure 1). For basic research, LF2000 is often used to transfect plasmid DNA or siRNA to analyze gene function in various cultured cell lines. We, therefore, compared with a commercially available transfection reagent, LF2000; however, luciferase activity was very low (Figure 1). Figure 2 shows the transfection efficiency using DsRed expressing plasmid DNA. The numbers of DsRed-positive cells markedly increased with the combination of BL and US exposure compared to the group treated with pDNA plus US or LF2000. It may be difficult to achieve efficient gene transfection to primary cultured cells by LF2000, because a low level of transfection efficiency in human umbilical vein endothelial cells (HUVEC) was also observed (data not shown). Our previous report showed that when the intracellular localization of fluorescent-labeled siRNA in COS7 cells just after transfection with BL and US exposure is examined by confocal laser scanning microscopy (CLSM) analysis, significant cytoplasmic distribution of siRNA can be observed [25]. Consequently, we concluded that unlike the transfection method with LF2000 involving endocytosis, transfection with BL and US does not involve endocytosis, but siRNA was directly and quickly introduced into the cytoplasm by physical force. Similarly, when fluorescent-labeled plasmid DNA was delivered to COS7 cells by the combination of BL and US exposure, plasmid DNA could

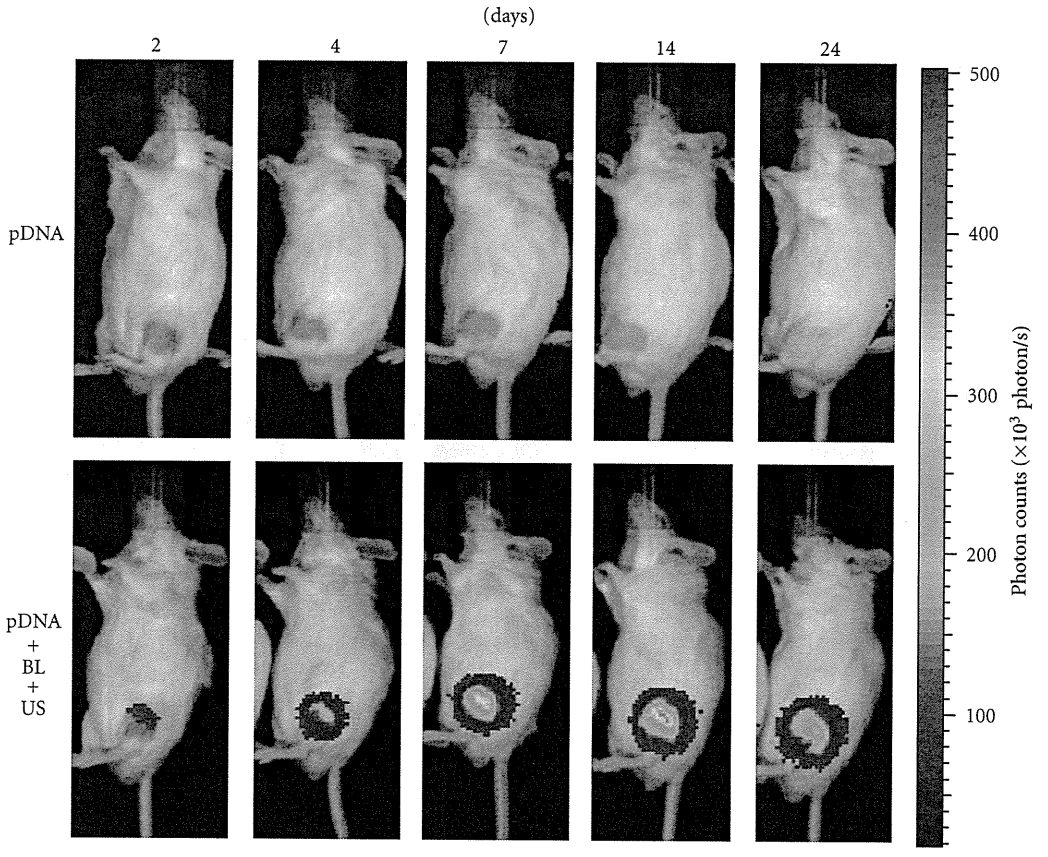

FIGURE 6: *In vivo* luciferase imaging. A suspension of pDNA and BL was injected into the knee joint of the mice, and US exposure (frequency, 1 MHz; duty, 50%; intensity, 2 W/cm^2; time, 60 sec) was immediately applied at the injection site. Luciferase expressions after transfection into the joint treated with pDNA, or pDNA plus BL plus US exposure were observed with an *in vivo* luciferase imaging system for 2–24 days.

be also distributed in the cytoplasm and nucleus (data not shown). Therefore, these results suggested that the combination of BL and US exposure facilitated the efficient transfection of pDNA into the cells due to the induction of cavitation.

Previously, our report demonstrated that gene transfection efficiency *in vitro* could be affected by increasing the US exposure time and intensity [22, 23]. We, therefore, examined the effect of US exposure time and intensity on transfection with BL into HFLS. High gene expression could be achieved by only 5 seconds of US exposure. In contrast, gene expression fell with a longer exposure time, 60 sec. (Figure 3), which might have been due to cytotoxicity. When we applied a range of US intensity (0.1–4 W/cm^2) in transfection, US intensity of 2.5 W/cm^2 was modestly higher than other treated groups (Figure 4). These results suggest that BL with US exposure is a useful gene delivery tool for *in vitro* transfection in synoviocytes.

3.2. Gene Transfection with Bubble Liposomes and Ultrasound Exposure into Joint Synovium In Vivo. A local gene delivery system to the joint synovium by BL and US exposure may be easily applied, because the injected BL may be retained in the confined joint space and percutaneous US exposure may induce cavitations on the surface of the synovium. We, therefore, attempted to deliver pCMV-Luc, luciferase-expressing plasmid DNA, into the joint synovium of mice using BL and US and to determine the level of the gene expression. A 40 μL solution of pDNA and BL was injected into the knee joint of the mice, and US exposure was immediately applied at the injection site. As a result, marked gene expression could be enhanced efficiently only with the combination of BL and US exposure when compared with other treatments (Figure 5). Exceeding our expectations, their gene expression was 500-fold higher than pDNA injection alone. We also observed luciferase gene expression area in the whole body using an *in vivo* luciferase imaging system during 2–24 days after transfection into a joint treated with pDNA, BL, and US exposure. The high level of gene expression persisted for 7–24 days after transfection using BL and US exposure (Figure 6). Gene expression was restricted to the area of US exposure. In contrast, no signal in the whole body was observed in the group with pDNA injection alone. This suggested that the combination of BL and US exposure facilitated the efficient transfection of pDNA into the joint tissue due to the induction of cavitation. We next investigated the localization of the transfected gene expression in the transfected joint by immunohistochemical analysis. This showed that the luciferase protein expression was limited to the synovial fibroblasts in the joint space. No

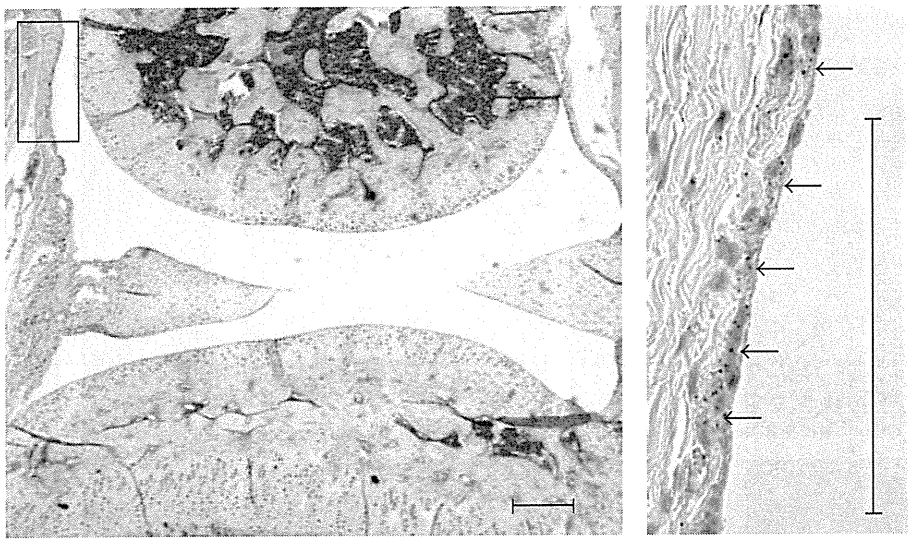

(a) (b)

FIGURE 7: Immunostaining for luciferase in synovial fibroblast. Local gene expression in joint synovium after intra-articular gene delivery using BL and US. Seven days after treatment, the expression of luciferase protein was mostly limited to the synovial fibroblasts. (a) H&E staining in joint sections. (b) Immunohistochemical localization of luciferase (arrows). Scale bar = 100 μm.

expression was observed in other tissues such as articular cartilage (Figure 7).

Gene transfer into cartilage may be difficult because cavitation induction with BL and US cannot reach chondrocytes embedded in extracellular matrix in articular cartilage, leading to no transfection. However, successful gene transfection into chondrocytes might be achieved by BL and US exposure, because articular chondrocytes in RA or OA are exposed by degradation of the extracellular matrix in articular cartilage in this stage of the disease.

It is known that cartilage degradation is the main pathological feature in OA; however, synovial factors are closely related to this progress [28], while synovitis is the main pathological feature of RA. Therefore, intra-articular gene therapy by BL and US exposure could be considered a feasible technique to deliver therapeutic proteins to suppress inflammation and destruction of the joints in RA and OA, because it could minimize extra-articular adverse effects linked to systemic injection of drugs; however, further study will be required for their assessment.

4. Conclusions

In this study, we showed that the combination of BL and US exposure could be an effective gene delivery method into synoviocytes *in vitro* and the joint synovium *in vivo*. In the future, this local gene delivery method with BL and US exposure might be used in non-viral gene therapy for joint disorders, such as RA and OA.

Acknowledgments

The authors are grateful to Dr. Katsuro Tachibana (Department of Anatomy, School of Medicine, Fukuoka University) for technical advice regarding the induction of cavitation with US and to Mr. Yasuhiko Hayakawa, Mr. Takahiro Yamauchi, and Mr. Kosho Suzuki (NEPA GENE CO., LTD.) for technical advice regarding US exposure. This study was supported in part by the Industrial Technology Research Grant Program (no. 04A05010) from New Energy, the Industrial Technology Development Organization (NEDO) of Japan, a Grant-in-Aid for Scientific Research (B) (no. 20300179) from the Japan Society of the Promotion of Science, and a grant for private universities provided by the Promotion and Mutual Aid Corporation for Private Schools of Japan. Y. Negishi and Y. Tsunoda contributed equally to this paper.

References

[1] C. H. Evans, P. D. Robbins, S. C. Ghivizzani et al., "Gene transfer to human joints: progress toward a gene therapy of arthritis," *Proceedings of the National Academy of Sciences of the United States of America*, vol. 102, no. 24, pp. 8698–8703, 2005.

[2] C. H. Evans, E. Gouze, J. N. Gouze, P. D. Robbins, and S. C. Ghivizzani, "Gene therapeutic approaches-transfer in vivo," *Advanced Drug Delivery Reviews*, vol. 58, no. 2, pp. 243–258, 2006.

[3] D. G. Miller, E. A. Rutledge, and D. W. Russell, "Chromosomal effects of adeno-associated virus vector integration," *Nature Genetics*, vol. 30, no. 2, pp. 147–148, 2002.

[4] M. Fechheimer, J. F. Boylan, S. Parker, J. E. Sisken, G. L. Patel, and S. G. Zimmer, "Transfection of mammalian cells with plasmid DNA by scrape loading and sonication loading," *Proceedings of the National Academy of Sciences of the United States of America*, vol. 84, no. 23, pp. 8463–8467, 1987.

[5] M. W. Miller, D. L. Miller, and A. A. Brayman, "A review of in vitro bioeffects of inertial ultrasonic cavitation from a

mechanistic perspective," *Ultrasound in Medicine and Biology*, vol. 22, no. 9, pp. 1131–1154, 1996.

[6] M. Joersbo and J. Brunstedt, "Protein synthesis stimulated in sonicated sugar beet cells and protoplasts," *Ultrasound in Medicine and Biology*, vol. 16, no. 7, pp. 719–724, 1990.

[7] W. J. Greenleaf, M. E. Bolander, G. Sarkar, M. B. Goldring, and J. F. Greenleaf, "Artificial cavitation nuclei significantly enhance acoustically induced cell transfection," *Ultrasound in Medicine and Biology*, vol. 24, no. 4, pp. 587–595, 1998.

[8] P. Schratzberger, J. G. Krainin, G. Schratzberger et al., "Transcutaneous ultrasound augments naked DNA transfection of skeletal muscle," *Molecular Therapy*, vol. 6, no. 5, pp. 576–583, 2002.

[9] M. Duvshani-Eshet and M. Machluf, "Therapeutic ultrasound optimization for gene delivery: a key factor achieving nuclear DNA localization," *Journal of Controlled Release*, vol. 108, no. 2-3, pp. 513–528, 2005.

[10] M. Duvshani-Eshet and M. Machluf, "Therapeutic ultrasound optimization for gene delivery: a key factor achieving nuclear DNA localization," *Journal of Controlled Release*, vol. 108, no. 2-3, pp. 513–528, 2005.

[11] H. J. Kim, J. F. Greenleaf, R. R. Kinnick, J. T. Bronk, and M. E. Bolander, "Ultrasound-mediated transfection of mammalian cells," *Human Gene Therapy*, vol. 7, no. 11, pp. 1339–1346, 1996.

[12] Y. Taniyama, K. Tachibana, K. Hiraoka et al., "Development of safe and efficient novel nonviral gene transfer using ultrasound: enhancement of transfection efficiency of naked plasmid DNA in skeletal muscle," *Gene Therapy*, vol. 9, no. 6, pp. 372–380, 2002.

[13] Y. Taniyama, K. Tachibana, K. Hiraoka et al., "Local delivery of plasmid DNA into rat carotid artery using ultrasound," *Circulation*, vol. 105, no. 10, pp. 1233–1239, 2002.

[14] T. Li, K. Tachibana, M. Kuroki, and M. Kuroki, "Gene transfer with echo-enhanced contrast agents: comparison between albunex, optison, and levovist in mice—initial results," *Radiology*, vol. 229, no. 2, pp. 423–428, 2003.

[15] E. C. Unger, T. Porter, W. Culp, R. Labell, T. Matsunaga, and R. Zutshi, "Therapeutic applications of lipid-coated microbubbles," *Advanced Drug Delivery Reviews*, vol. 56, no. 9, pp. 1291–1314, 2004.

[16] S. Sonoda, K. Tachibana, E. Uchino et al., "Gene transfer to corneal epithelium and keratocytes mediated by ultrasound with microbubbles," *Investigative Ophthalmology and Visual Science*, vol. 47, no. 2, pp. 558–564, 2006.

[17] G. Blume and G. Cevc, "Liposomes for the sustained drug release in vivo," *Biochimica et Biophysica Acta*, vol. 1029, no. 1, pp. 91–97, 1990.

[18] T. M. Allen, C. Hansen, F. Martin, C. Redemann, and A. F. Yau-Young, "Liposomes containing synthetic lipid derivatives of poly(ethylene glycol) show prolonged circulation half-lives in vivo," *Biochimica et Biophysica Acta*, vol. 1066, no. 1, pp. 29–36, 1991.

[19] K. Maruyama, T. Yuda, A. Okamoto, S. Kojima, A. Suginaka, and M. Iwatsuru, "Prolonged circulation time in vivo of large unilamellar liposomes composed of distearoyl phosphatidylcholine and cholesterol containing amphipathic poly(ethylene glycol)," *Biochimica et Biophysica Acta*, vol. 1128, no. 1, pp. 44–49, 1992.

[20] K. Maruyama, O. Ishida, S. Kasaoka et al., "Intracellular targeting of sodium mercaptoundecahydrododecaborate (BSH) to solid tumors by transferrin-PEG liposomes, for boron neutron-capture therapy (BNCT)," *Journal of Controlled Release*, vol. 98, no. 2, pp. 195–207, 2004.

[21] Y. Negishi, D. Omata, H. Iijima et al., "Preparation and characterization of laminin-derived peptide AG73-coated liposomes as a selective gene delivery tool," *Biological and Pharmaceutical Bulletin*, vol. 33, no. 10, pp. 1766–1769, 2010.

[22] R. Suzuki, T. Takizawa, Y. Negishi et al., "Gene delivery by combinationof novel liposomal bubbles with perfluoropropane and ultrasound," *Journal of Controlled Release*, vol. 117, no. 1, pp. 130–136, 2007.

[23] R. Suzuki, T. Takizawa, Y. Negishi et al., "Tumor specific ultrasound enhanced gene transfer in vivo with novel liposomal bubbles," *Journal of Controlled Release*, vol. 125, no. 2, pp. 137–144, 2008.

[24] R. Suzuki, T. Takizawa, Y. Negishi, N. Utoguchi, and K. Maruyama, "Effective gene delivery with novel liposomal bubbles and ultrasonic destruction technology," *International Journal of Pharmaceutics*, vol. 354, no. 1-2, pp. 49–55, 2008.

[25] Y. Negishi, Y. Endo, T. Fukuyama et al., "Delivery of siRNA into the cytoplasm by liposomal bubbles and ultrasound," *Journal of Controlled Release*, vol. 132, no. 2, pp. 124–130, 2008.

[26] Y. Negishi, D. Omata, H. Iijima et al., "Enhanced laminin-derived peptide AG73-mediated liposomal gene transfer by bubble liposomes and ultrasound," *Molecular Pharmaceutics*, vol. 7, no. 1, pp. 217–226, 2010.

[27] R. Suzuki, E. Namai, Y. Oda et al., "Cancer gene therapy by IL-12 gene delivery using liposomal bubbles and tumoral ultrasound exposure," *Journal of Controlled Release*, vol. 142, no. 2, pp. 245–250, 2010.

[28] J. C. Fernandes, J. Martel-Pelletier, and J. P. Pelletier, "The role of cytokines in osteoarthritis pathophysiology," *Biorheology*, vol. 39, no. 1-2, pp. 237–246, 2002.